

**Eta-CMAQ air quality forecasts for O₃ and related species using
three different photochemical mechanisms (CB4, CB05, SAPRC-99):
Comparisons with measurements during the 2004 ICARTT study**

Shaocai Yu, Rohit Mathur, Golam Sarwar, Daiwen Kang^{*},
Daniel Tong⁺, George Pouliot, Jonathan Pleim

Atmospheric Modeling and Analysis Division
National Exposure Research Laboratory, U.S. Environmental Protection Agency,
Research Triangle Park, NC 27711

^{*}Computer Science Corporation, Research Triangle Park,
79 T.W. Alexander Drive, NC 27709

⁺Science and Technology Corporation,
1315 East West Highway, Silver Spring, MD 20910

To be revised to

Atmospheric Chemistry and Physics

Abstract

A critical module of air quality models is the photochemical mechanism. In this study, the impact of the three photochemical mechanisms (CB4, CB05, SAPRC-99) on the Eta-Community Multiscale Air Quality (CMAQ) model's forecast performance for O_3 , and its related precursors has been assessed over the eastern United States with observations obtained by aircraft (NOAA P-3 and NASA DC-8) flights, ship and two surface networks (AIRNow and AIRMAP) during the 2004 International Consortium for Atmospheric Research on Transport and Transformation (ICARTT) study. The results show that overall none of the mechanisms performs systematically better than the others. On the other hand, at the AIRNow surface sites, CB05 has the best performance with the normalized mean bias (NMB) of 3.9%, followed by CB4 (NMB=-5.7%) and SAPRC-99 (NMB=10.6%) for observed $O_3 \geq 75$ ppb, whereas CB4 has the best performance with the least overestimation for observed $O_3 < 75$ ppb. On the basis of comparisons with aircraft P-3 measurements, there were consistent overestimations of O_3 , NO_x , PAN and NO_y and consistent underestimations of CO, HNO_3 , NO_2 , NO, SO_2 and terpenes for all three mechanisms although the NMB values for each species and mechanisms were different. The results of aircraft DC-8 show that CB05 predicts the H_2O_2 mixing ratios most closely to the observations (NMB=10.8%), whereas CB4 and SAPRC-99 overestimated (NMB=74.7%) and underestimated (NMB=-25.5%) H_2O_2 mixing ratios significantly, respectively. For different air mass flows over the Gulf of Maine on the basis of the ship data, the three mechanisms have relatively better performance for O_3 , isoprene and SO_2 for the clean marine or continental flows but relatively better performance for CO, NO_2 and NO for southwest/west offshore flows. The results of the O_3 - NO_x slopes over the ocean indicate that SAPRC-99 has the highest upper limits of the ozone production efficiency (ϵ_N) (5.8), followed by CB05 (4.5) and CB4 (4.0) although they are much lower than that inferred from the observation (11.8), being consistent with the fact that on average, SAPRC-99 produces the highest O_3 , followed by CB05 and CB4, across all O_3 mixing ratio ranges

1. Introduction

One of the most important components of air quality models (AQMs) is the photochemical mechanism which describes how volatile organic compounds (VOCs) and oxides of nitrogen (NO_x) interact to produce O_3 and other oxidants. Photochemical mechanisms were first used in AQMs more than 30 years ago (e.g., Reynolds et al., 1973). Highly detailed and explicit photochemical mechanisms such as the Master Chemical Mechanism (MCM) (Jenkin et al., 1997), which includes over 2400 chemical species and over 7100 chemical reactions for 120 of the most important emitted organic compounds, exist. The chemistry of atmospheric systems involves reactions whose characteristic time scales vary by orders of magnitude, resulting in a set of nonlinear stiff ordinary differential equations (ODEs), the numerical integration of which often comprises a large fraction of the overall chemical transport model computational time (Mathur et al., 1998; McRae et al., 1982). Thus, for practical reasons, the representation of photochemical mechanism in AQMs employs different methods including various types of parameterizations, approximations and condensations (Dodge, 2000). Uncertainties in the model's chemical mechanisms can range to 30% or more when new techniques are applied to re-measure reaction rate constants and yields (Russell and Dennis, 2000).

Three of the most commonly used chemical mechanisms in current AQMs for both regulatory and research applications include the Carbon Bond 4 (CB4) (Gery et al., 1989), SAPRC-99 (Carter, 2000) and CB05 (an update to CB4, Yarwood et al., 2005). All three mechanisms have been evaluated against measurements from a large number of chamber experiments and have been demonstrated to be reasonably successful in predicting ozone and related species from complex mixtures in "typical" urban atmospheres (Gery et al., 1989, Yarwood et al., 2005, Carter, 2000). The Carbon Bond (CB) mechanisms mostly use the lumped structure technique to condense the reactions of individual VOCs, whereas the SAPRC mechanism uses the lumped molecule technique to condense VOCs. In the lumped molecule technique, a generalized or surrogate species is used to represent similar organic compounds, whereas in the lumped structure technique, organic compounds are grouped according to bond type. Given the fact that different chemical schemes can have different formulations of the reaction mechanism, different rate constants and temperature and pressure dependencies for the reactions (Kuhn et al., 1998),

it is not surprising that they sometimes yield different results. Several intercomparison studies of different chemical mechanisms have been performed with box and trajectory models, and 3-D AQMs over the last decade and the results have been summarized in detail by many investigators (Dunker et al., 1984; Stockwell, 1986; Jimenez et al., 2003; Gross and Stockwell, 2003; Kuhn et al., 1998; Luecken et al., 1999, 2008). For example, with box model calculation, Jimenez et al. (2003) compared seven different photochemical mechanisms (including LCC, CBM-IV, RADM2, EMEP, RACM, SAPRC-99 and CACM) and indicated that most chemical schemes yield similar O₃ mixing ratios. However, they also found significant discrepancies, mainly in predicted mixing ratios of HNO₃, HO₂ and total PAN among the model simulations, even under extremely simple situations. With the simulations of 3-D AQMs, Faraji et al. (2008) compared CB4 and SAPRC-99 in southeast Texas and found that for most urban areas, the CB4 and SAPRC-99 mechanisms yield similar results, but for 2000 summer in southeast Texas, the SAPRC-99 mechanism leads to O₃ mixing ratios that are 30-45 ppb higher than CB4. Faraji et al. (2008) attributed these discrepancies to differences in both reaction rate/stoichiometry parameters and condensation methods in the mechanisms. On the other hand, Luecken et al. (2008) recently examined the differences in predictions of O₃ and its O₃ precursors among CB4, CB05 and SAPRC-99 in a 3-D MM5-CMAQ model over the continental US. They show that the predicted O₃ mixing ratios are similar for most of the US, but statistically significant differences occur over many urban areas and the central US among the predictions by the three mechanisms, depending on location, the VOC/NO_x ratio, and precursor concentrations. They also found that on average, SAPRC-99 predicts the highest O₃, followed by CB05 and CB4.

In this study, we compare the CB4, CB05 and SAPRC-99 mechanisms by examining the impact of these different chemical mechanisms on the Eta-CMAQ air quality forecast model simulations for O₃ and its related precursors over the eastern US through comparisons with the intensive observational data obtained during the 2004 International Consortium for Atmospheric Research on Transport and Transformation (ICARTT) study. The 2004 ICARTT experiment provided a comprehensive set of measurements of chemical constituents, both from surface and aircraft based platforms, which can be used to examine in detail the impact of chemical mechanisms from a multi-pollutant

perspective, both in terms of their surface concentrations as well as vertical structure. This aspect constitutes the primary difference of this study from the previous comparative analyses of these mechanisms. The objective of this study is to assess the influence of the three photochemical mechanisms on the Eta-Community Multiscale Air Quality (CMAQ) model's ability to simulate O_3 , its related chemical species over the eastern United States with observations obtained by aircraft (NOAA P-3 and NASA DC-8) flights, ship and two surface networks (AIRNow and Atmospheric Investigation, Regional Modeling, Analysis, and Prediction (AIRMAP)) during the 2004 International Consortium for Atmospheric Research on Transport and Transformation (ICARTT) study.

2. Description of the photochemical mechanisms, Eta-CMAQ model and observation database

2.1. Photochemical mechanisms

Detailed description of the CB4, CB05 and SAPRC-99 chemical mechanisms (species and reaction rates) and their evaluations against smog chamber experimental data can be found in Gery et al. (1989), Yarwood et al. (2005) and Carter (2000), respectively. Luecken et al. (2008) previously summarized the general characteristics of the three mechanisms used in this study; a brief summary relevant to this study is presented here. The version of CB4 in CMAQ (<http://www.cmaq-model.org>) has 46 species (30 organic species) and 96 reactions (45 inorganic reactions). In contrast, CB05, an updated version of the CB4, includes 59 species and 156 reactions, with updated reaction rate constants, additional inorganic reactions and more organic species relative to CB4. Both CB4 and CB05 mostly use the lumped-structure technique to condense the organic chemistry. On the other hand, SAPRC-99 has 80 species and 214 reactions and uses a lumped molecule approach to condense the organic chemistry, i.e., surrogate species are used to represent similar organic compound. Tables 1 and 2 compare the reaction rates of inorganic and organic species at 298 K and 1 atmosphere, respectively, for the three mechanisms. Inorganic chemistry describes the chemistry of O_3 , various NO_x species, H_2O_2 , OH and HO_2 radicals, CO, HNO_3 , HNO_2 , HNO_4 and PNA. Organic chemistry includes the chemistry of formaldehyde, higher molecular weight aldehydes, alkanes, alkenes, aromatics, isoprene, terpene, ketone, and other organic compounds. As

can be seen, there are many differences among CB4, CB05 and SAPRC-99 chemical mechanisms. SAPRC-99 includes more detailed organic chemistry than Carbon Bond mechanisms as SAPRC-99 was developed with the additional capability of representing reactions of a wide variety of individual VOCs (Carter, 1999). Updates to inorganic chemistry in CB05 compared to CB4 mechanism include (Yarwood et al., 2005): (1) updated rate constants based on recent (2003-2005) IUPAC and NASA evaluations, (2) an extended inorganic reaction set for urban to remote tropospheric conditions, (3) NO_x recycling reactions to represent the fate of NO_x over multiple days. Updates to organic chemistry in CB05 compared to CB4 mechanism include (Yarwood et al., 2005): (1) explicit organic chemistry for methane and ethane, (2) explicit methylperoxy radical, methyl hydroperoxide and formic acid, (3) lumped higher organic peroxides, organic acids and peracids, (4) internal olefin (R-HC=CH-R) species called IOLE, (5) higher aldehyde species ALDX, making ALD2 explicitly acetaldehyde, (6) higher peroxyacyl nitrate species from ALDX called PANX. As analyzed by Luecken et al. (2008), the reasons for CB05 to produce more O₃ relative to CB4 include (1) the ALDX (aldehydes with more than two carbons) species in CB05 can produce about 50% more conversions of NO to NO₂, (2) the photolysis rate of ALDX in CB05 is higher compared to ALD2, leading to higher production of HO_x, (3) the additional acyl peroxy radicals (CXO3) in CB05 (e.g., CB05 uses two species (acetyl peroxy radical (C2O3) and other acyl peroxy radicals (CXO3) while CB4 only uses one species to represent all acyl peroxy radicals (C2O3)) can produce 50% more conversions of NO to NO₂ than C2O3; this effect is apparent in the reactions of alkenes, including isoprene, with O₃ and NO₃, (4) CB05 uses methyl peroxy radical (MEO2) to replace the alkyl peroxy radical operator (XO2) in some reactions to better represent reactions under low NO_x conditions, (5) CB05 adds a model species to represent internal alkenes, which are allowed to react with O₃ and can change the temporal production of O₃, (6) CB05 allows HNO₃ and organic nitrate to photolyze and produce HO_x and NO₂, providing additional organic radicals.

2.2. Eta-CMAQ forecast model

The developmental Eta-CMAQ air quality forecasting system for O₃, created by linking the Eta model (Rogers et al., 1996) and the CMAQ modeling system (Byun and

Schere, 2006), was applied over a domain encompassing the eastern U.S. (see Figure 1) during summer 2004. The detailed description of model configurations can be found in Yu et al. (2007). The Eta model provided the meteorological fields for input to CMAQ. The model domain has a horizontal grid spacing of 12 km with twenty-two vertical layers between the surface and 100 mb. The boundary conditions for various species were based on a static vertical profile that was uniformly applied along all lateral boundaries. The species profiles are representative of continental “clean” conditions except O₃ whose lateral boundary conditions are derived from the Global Forecast System (GFS) model. The primary Eta-CMAQ model forecast for next-day is based on the current day’s 12 UTC Eta simulation cycle. The area source emissions are based on the 2001 National Emission Inventory (NEI). The point source emissions are based on the 2001 NEI with SO₂ and NO_x projected to 2004 on a regional basis using the Department of Energy’s 2004 Annual Energy Outlook issued in January of 2004. The mobile source emissions were generated by EPA’S MOBILE6 model using 1999 vehicle miles traveled (VMT) data and a fleet year of 2004. Daily temperatures from the Eta model were used to drive the inputs into the MOBILE6 model using a nonlinear least squares relationship described in Pouliot [2005]. The biogenic emissions are calculated using Biogenic Emissions Inventory System (BEIS) version 3.12. The CB4, CB05 and SAPRC-99 chemical mechanisms as described in section 2.2 have been used to represent photochemical reaction pathways in the three cases.

2.3. Observation database

The hourly, near real-time observed O₃ data at 614 sites in the eastern U.S. are available from the U.S. EPA’s AIRNow (Figure 1) for the study period. Note that AIRNow data have only gone through some preliminary data quality assessments. From July 1 to August 15, 2004, measurements of vertical profiles of O₃ and its related chemical species (CO, NO, NO₂, H₂O₂, CH₂O, HNO₃, SO₂, PAN, isoprene, terpenes) were carried out by instrumented aircraft (NOAA P-3 and NASA DC-8) deployed as part of the 2004 ICARTT field experiment. The observations of O₃ and its related chemical species along the coast of New Hampshire, Massachusetts and Maine were obtained by the NOAA ship Ronald H. Brown during the 2004 ICARTT field experiment. The

detailed instrumentation and protocols for measurements are described in <http://www.al.noaa.gov/ICARTT/FieldOperations/>. The flight tracks of P-3, DC-8, and ship are presented in Figure 2. Four sites of the AIRMAP (DeBell et al., 2004; Mao and Talbot, 2004) provided continuous measurements of O₃ and related photochemical species as well as meteorological parameters during the study; the sites include Castle Springs (CS) (43.73°N, 71.33°W), New Hampshire (NH), Isle of Schoals (IS) (42.99°N, 69.33°W), Maine, Mount Washington Observatory (MWO) (44.27°N, 71.30°W), NH, and Thompson Farm (TF) (43.11°N, 70.95°W), NH. The comparison of the model results for the three mechanisms during the period of July 15-August 18, 2004 is examined in this study.

3. Results and discussion

3.1. O₃ comparison at the AQS sites

To gain insights into the model performance, the normalized mean bias (NMB) values (Yu et al., 2006) for maximum 8-hr O₃ as a function of the different observed O₃ mixing ratio ranges are calculated for the three mechanisms and are displayed in Figure 3. As can be seen, for O₃ mixing ratios greater than 75 ppb, CB05 exhibits the best performance with the NMB of 3.9%, followed by CB4 (NMB=-5.7%) and SAPRC-99 (NMB=10.6%). In contrast, for O₃ mixing ratios less than 75 ppb, CB4 exhibited the least overestimation amongst the three mechanisms; CB05 and SAPRC-99 produce more O₃ than CB4 for all O₃ mixing ratio ranges (see Figure 3). As analyzed by Yu et al. (2007), one of the reasons for the overestimation of observations in the low O₃ mixing ratio ranges could be indicative of titration by NO in urban plumes that the model does not resolve because majority of the AIRNow sites are located in urban or suburban areas. Another one is because of the significant overestimation in areas of cloud cover mainly caused by the unrealistic vertical transport of excessive amounts of high O₃ concentrations near the tropopause to the ground associated with downward entrainment in CMAQ's convective cloud scheme (Yu et al., 2007). The spatial distributions of NMB values indicate that large overestimation of the observed daily max 8-hr O₃ mixing ratios was in the northeast for all three mechanisms where very low O₃ mixing ratios were

observed for all three mechanisms (not shown). Spatially, SAPRC-99 is more similar to CB05 with the exception that SAPRC-99 has slightly more overpredictions.

3.2. Vertical profile comparisons for different species

To compare the modeled and observed vertical profiles, the observed and modeled data were grouped according to the model layer for each day and each flight: that is, both observations and predictions were averaged along the aircraft transect according to layer height, representing the average conditions encountered over the study area. The aircraft flight tracks in Figure 2 show that observations onboard the P-3 cover a regional area over the northeast around NY and Boston, whereas the DC-8 aircraft covers a broader regional area over the eastern U.S. Figures 4-6 present observed and modeled (CB4, CB05, SAPRC-99) vertical profiles for O₃, CO, SO₂, NO_x, NO, NO₂, HNO₃, NO_y, NO₂+O₃, HCHO, terpenes, isoprene, PAN, and H₂O₂ on the daily basis during the 2004 ICARTT period. Table 3 summarizes the results of comparison for all observation and model data during the 2004 ICARTT period.

As shown in Figures 4 and 6, and Table 3, all three mechanisms tend to consistently overestimate O₃ from low altitude to high altitude with the highest for SAPRC-99, followed by CB05 and CB4, similar to trends noted relative to AIRNow measurement at the surface, although they reproduce the vertical variation patterns of O₃ well. All three mechanisms tend to overestimate more in the upper layers at altitude >6 km on the basis of DC-8 observations (see Figure 6) due to effects of the lateral boundary conditions derived from the Global Forecast System (GFS) model and coarse vertical model resolution in the free troposphere (Yu et al., 2007). Figures 4-6 and Table 3 also indicate that there are many noticeable consistencies and discrepancies for different species among the three chemical mechanisms. Noticeable among these are consistent overestimations of O₃, NO_z, PAN, NO_y, and O₃+NO₂ and consistent underestimations of CO, HNO₃, NO₂, NO, SO₂, and terpenes relative to the P3 observations. There were consistent overestimations of O₃, HNO₃, and HCHO and consistent underestimations of CO, NO₂, SO₂, and NO relative to DC-8 observations for all three mechanisms although the NMB values for each species and mechanism are somewhat different as listed in Table 3. One reason for the consistent underestimations of CO relative to both P3 and

DC8 observations for the three model configurations can be the inadequate representation of the transport of pollution associated with biomass burning from outside the domain, especially from large Alaska forest fires during this period (Yu et al., 2007; Mathur, 2008).

In terms of the NMB values for each species relative to P3 observations in Table 3, CB4 has relatively better performance for O_3 and HNO_3 , whereas CB05 has the relatively better performance for CO, NO_2 , and NO_x , and SAPRC-99 has the relatively better performance for SO_2 . The speciation of NO_y in the different mechanisms is different, i.e., CB4: $NO_y = NO + NO_2 + NO_3 + 2N_2O_5 + HONO + HNO_3 + PAN + PNA + NTR$, CB05: $NO_y = NO + NO_2 + NO_3 + 2N_2O_5 + HONO + HNO_3 + PAN + PNA + NTR + PANX$, and SAPRC-99: $NO_y = NO + NO_2 + NO_3 + 2N_2O_5 + HONO + HNO_3 + HNO_4 + PAN + PAN2 + PBZN + MA_PAN + BZNO2_O + NPHE$. Despite the fact that CB4 apportions PAN (peroxyacetyl nitrate) and homologs (peroxyprionyl nitrate and larger compounds) differently from the CB05 and SAPRC-99 (Luecken et al., 2008), both CB4 and CB05 overestimated observed PAN from low to high altitudes (see Figure 5) by about a factor of 2 while SAPRC-99 results are more close to the observations (see Table 3). Henderson et al. (2009) suggested several reasons for model over-prediction of PAN; possible reasons include the uncertainty in the reaction rate of per-acetic acid with hydroxyl radicals, over-estimation of acetone photolysis, the omission of PAN photolysis, and omission of hydroxyl reaction with PAN. There are consistent underestimations of NO_x relative to both P3 and DC-8 observations (See Table 3 and Figures 4 and 6) for all three mechanisms, being in agreement with Singh et al. (2007). This is likely due to the fact that the aircraft and lightning NO emissions are not included in the current model emission inventory. Ridley et al. (2005) suggested that cloud-to-cloud discharges may be a far greater source of NO_x than what has traditionally been believed. The three mechanisms slightly underestimated HNO_3 relative to P3 observations while they slightly overestimated HNO_3 relative to DC-8 observation as shown in Table 3. One of the reasons for this different performance is because of different areas measured by P3 and DC-8 as shown in Figure 2.

On the basis of DC-8 observations, CB05 performs relatively better for H_2O_2 and CO than CB4 and SAPRC-99. H_2O_2 and hydroperoxide radical (HO_2) are photochemical

products and are affected by the levels of chemical components such as NO_x , CO, methane and non-methane hydrocarbons (Lee et al., 2000). Kuhn et al. (1998) pointed out that H_2O_2 and organic peroxides chemistry is a weak point in most mechanisms due to the fact that there are many complex reactions and possibly important unknowns like the incorrect use of the $\text{HO}_2 + \text{HO}_2$ rate constant and different treatment of the peroxy radical interactions. Among the three mechanisms, the H_2O_2 mixing ratios from CB05 are the closest to the observations with a NMB value of 10.8%, whereas CB4 significantly overestimated the H_2O_2 mixing ratios from low to high altitudes (see Figure 6) with the NMB value of 74.7% (see Table 3) due to the fact that the H_2O_2 formation rate in CB4 is 62% higher than CB05 or SAPRC-99 (Luecken et al., 2008). On the other hand, SAPRC-99 underestimated H_2O_2 mixing ratios with a NMB value of -25.5%. Compared to SAPRC-99, CB05 can produce more new HO_2 , enhancing formation of H_2O_2 as pointed out by Luecken et al. (2008). In addition, Table 3 shows that on the basis of DC-8 observations, CB4 has relatively better performance for O_3 , whereas CB05 has the relatively better performance for HNO_3 and SO_2 , and SAPRC-99 has the relatively better performance for HCHO and NO. The different model performance for the same species relative to P3 and DC-8 observations can be attributed to the difference in the studying areas of P3 and DC-8 as indicated in Figure 2.

Biogenic monoterpene and isoprene emission rates are high over the coniferous forests of northeastern North America, especially in the summer months (Guenther et al., 2000). Isoprene is the most significant biogenic compound regarding photochemistry and terpene is a significant gas precursor for the formation of biogenic secondary organic aerosols (SOA). Isoprene is highly reactive in the atmosphere with a relatively short lifetime compared to other reactive VOCs. Table 2 shows that all three mechanisms consider the reactions of isoprene with atomic oxygen, OH radicals, NO_3 radicals, and O_3 although the reaction products and propagation reactions are different amongst the mechanisms. The results in Figure 5 show that the three mechanisms have similar performance for isoprene with significant overestimation at altitudes between ~200 and 300 m but slight underestimation above it. On average for all data as summarized in Table 3, CB05 has slightly better results for isoprene with the NMB value of 5.5%, whereas CB4 and SAPRC-99 have the negative NMB values of -6.0% and -8.4%,

respectively. A close inspection of Figure 5 shows that CB05 has slightly higher isoprene mixing ratios at the high altitudes (>Layer 5) than CB4 and SAPRC-99. On the other hand, the three mechanisms systematically underestimated the observed terpenes by more than a factor of 2 from low to high altitudes except at the layer 3 (~200 m) where the mean results of the three mechanisms are close to the observations due to high model terpenes mixing ratios at layer 3 on 7/22 when the P3 observations took place over the northeastern part as indicated in Figure 2. Improvement of the VOC emission inventory is recommended in order to provide better model results for these species. For instance, MEGAN (Guenther et al., 2006) provides different estimates for isoprene and other biogenic VOCs. Since MEGAN has higher isoprene estimates than BEIS and if the ozone production was VOC-limited, MEGAN would increase ozone. If ozone production is NO_x -limited, however, the differences in MEGAN and BEIS would have little impact on ozone.

3.3. Time series comparison over the ocean with the Ronald H. Brown ship observations

The cruise tracks of the NOAA ship Ronald H. Brown of Figure 2 shows that most of ship's cruising time was spent sampling along the coast of New Hampshire, Massachusetts and Maine. The time-series of observations and model predictions (CB4, CB05 and SAPRC-99) for different species (O_3 , O_3+NO_2 , CO, NO_y , NO_2 , NO, PAN, SO_2 , and isoprene) along the ship tracks during the ICARTT period are shown in Figure 7. As analyzed by Yu et al. (2007), the air mass flow patterns sampled in the Gulf of Maine can be divided into two groups for our study period: (1) offshore flows from the west and southwest that are significantly affected by anthropogenic sources from the Washington, D.C./New York City/Boston urban corridor and biogenic emissions in New Hampshire and Maine, and (2) relatively clean marine and continental flows from the east, south, north and northwest. On days with the southwesterly/westerly offshore flows such as 10 July, 15-17 July, and 20-23 July, 29 July to 1 August, 3-4 August, 8-12 August, and 16-17 August, measured concentrations for each species were clearly seen above the background values. The easterly/northerly/northwesterly/southerly clean marine or continental flows impacted the ship observations on days 11-13 July, 18 July, and 25-28

July and 5-7 August which were characterized by low mixing ratios of O₃, CO, NO_y, SO₂, and NO_x. Table 4 summarizes the mean results for these two different flows on the basis of wind fields observed by High-Resolution Doppler Lidar (HRDL) (Yu et al., 2007). As can be seen, all three mechanism model configurations exhibit relatively better model performance for the clean marine or continental flows for O₃, O₃+NO₂, isoprene, and SO₂ compared to southwesterly/westerly offshore flows. On the other hand, the three mechanisms exhibit relatively better model performance for CO, NO₂, and NO for southwesterly/westerly offshore flows. The clean marine or continental flows have significantly lower mixing ratios than the southwesterly/westerly polluted flows for all species except NO and PAN on the basis of observations. The three mechanisms have very similar performance for the clean marine or continental flows with general underestimations for all species except O₃ as shown in Table 4 due to the fact that the mixing ratios of all those species are close to the background in these clean flows. This similarity is also consistent with the use of the same boundary conditions for all simulations. In contrast, all three mechanisms exhibit consistent overestimations of SO₂, PAN, NO_y, and O₃ for the southwesterly/westerly polluted flows.

In terms of the NMB values for each species in Table 4, all three mechanisms reproduced the observations of CO, NO₂, and NO in the southwesterly/westerly polluted flows well with the NMB value $\leq \pm 20\%$. Comparing the results of Table 4 and 3 for each species, the model performance statistics for the southwesterly/westerly polluted flow conditions are similar to those for the aircraft measurement comparisons. For example, in the southwesterly/westerly polluted flows, all three mechanisms tend to consistently overestimate O₃ with the highest for SAPRC-99, followed by CB05 and CB4, and the three mechanisms tend to consistently overestimate NO_y and PAN with slightly better performance for SAPRC-99. Also noticeable in these comparisons is significant overestimation of SO₂ but underestimation of isoprene during the southwesterly/westerly polluted flows. This suggests that the CMAQ modeling system may have overestimated some of emission sources of SO₂ from urban plumes over Washington, D.C./New York City/Boston areas and underestimated biogenic emissions of isoprene on the basis of ship observations.

The upper limits of the ozone production efficiency (ϵ_N) values can be estimated by the O_3 - NO_z ($NO_z=NO_y-NO_x$) slope because NO_z species (primarily HNO_3) are removed from the atmosphere more rapidly than O_3 (Yu et al., 2007). Following Arnold et al. (2003), both modeled and observed O_3 - NO_z slopes are obtained for only observational data with $[O_3]/[NO_x]>46$. The results of Table 4 reveal that the ϵ_N values of the three mechanisms are much lower than the corresponding observation (11.8) with the highest for SAPRC-99 (5.8), followed by CB05 (4.5) and CB4 (4.0), whereas the intercepts of O_3 - NO_z relationships for the three mechanisms are higher than the observations, indicating that background O_3 mixing ratios in the model are too high. The ϵ_N values of SAPRC-99, CB05 and CB4 are consistent with the fact that SAPRC-99 produces the highest O_3 , followed by CB05 and CB4 as previously discussed. The overpredictions of NO_z mixing ratios indicate that all three chemical mechanisms still produce more terminal oxidized nitrogen products than inferred from observations, thereby contributing in part to the noted underestimation of ϵ_N .

3.4. Comparisons at the AIRMAP sites

Table 5 lists the comparison of observations and three mechanisms (CB4, CB05 and SAPRC-99) for different species (O_3 , CO, NO, NO_y , and SO_2) at the four AIRMAP (CS, IS, MWO and TF) sites on the basis of hourly time-series data during the 2004 ICARTT period. As can be seen, there are several consistent features in the model performance with of the three different mechanisms at each site. All three mechanisms underestimate NO, and CO but overestimate O_3 at all four sites. The three mechanisms consistently overestimated NO_y at the CS and TF sites but underestimated NO_y at the MWO site. Compared to the other sites, relatively poor model performance for several species is noted at the MWO site (the highest mountain (1916 m) in the northeastern U.S.). This, in part, arises from the inability of the model to capture the inherent sub-grid variability at this location. The models usually misrepresent mountain sites because they essentially sample free tropospheric air while the models can't resolve the terrain. Overall, CB4 has the smallest NMB values for O_3 based on the entire hourly data, whereas SAPRC-99 has the better results for NO_y at the CS and TF sites. This also is in agreement with the previous results of P-3.

4. Summary and conclusions

A rigorous comparison of the three photochemical mechanisms (CB4, CB05 and SAPRC-99) for the Eta-CMAQ air quality forecast model for O₃ and its related precursors has been carried out by comparing the model results with intensive observations over the eastern United States obtained during the 2004 ICARTT study. All the three photochemical mechanisms are used as part of the chemical transport model in the Eta-CMAQ air quality forecast model. The main conclusions of the comparison results are summarized below. The comparisons with measurements at the AIRNow surface sites show that SAPRC-99 predicts the highest O₃ mixing ratios, followed by CB05 and CB4 for all O₃ mixing ratio ranges and that relative to observations for the O₃ mixing ratios ≥ 75 ppb, CB05 has the best performance with NMB=3.9%, followed by CB4 (NMB=-5.7%) and SAPRC-99 (NMB=10.6%), whereas CB4 has the best performance for observed O₃ mixing ratios < 75 ppb. On the basis of vertical results from P-3 and DC-8 aircraft, all three mechanisms tend to consistently overestimate O₃ from low altitude to high altitude with the highest for SAPRC-99, followed by CB05 and CB4. On the basis of P-3 observations, there were consistent overestimations of O₃, NO_z, PAN, and NO_y, and consistent underestimations of CO, HNO₃, NO₂, NO, SO₂ and terpenes for the three mechanisms although the NMB values for each species and mechanism are somewhat different. On the basis of DC-8 observations, CB05 has relatively better performance for H₂O₂ and CO than CB4 and SAPRC-99. Among the three mechanisms, CB05 predictions of H₂O₂ are the closest to the observations with NMB=10.8%, whereas CB4 significantly overestimates H₂O₂ with NMB=74.7% and SAPRC-99 significantly underestimates H₂O₂ with NMB=-25.5%. This is due to the fact that the H₂O₂ formation rate in CB4 is 62% higher than CB05, and relative to SAPRC-99, CB05 can produce more new HO₂, enhancing formation of H₂O₂. On the basis of DC-8 observations, CB4 has relatively better performance for O₃, whereas CB05 has the relatively better performance for HNO₃ and SO₂, and SAPRC-99 has the relatively better performance for HCHO and NO. The three mechanisms overestimated isoprene below 300 m but slightly underestimated isoprene above 300 m. The three mechanisms

systematically underestimated the observed terpenes by more than a factor of 2 most of time.

The capability of the three mechanisms to reproduce the observed pollutant concentrations over the ocean areas (Gulf of Maine) was found to be dependent on the offshore flow types. The three mechanisms exhibit relatively better performance for O₃, isoprene and SO₂ for the clean marine or continental flows but relatively better performance for CO, NO₂ and NO for southwest/west offshore flows. Model performance during southwest/west polluted flow conditions was similar to that noted for aircraft measurements except isoprene. According to the ship data, the upper limits of the ozone production efficiency (ϵ_N) values estimated on the basis of the O₃-NO_x slope are 5.8, 4.5, and 4.0 for SAPRC-99, CB05 and CB4, respectively, much lower than the observation (11.8). This is also consistent with the fact that SAPRC-99 produces the highest O₃, followed by CB05 and CB4. The overpredictions of NO_x mixing ratios in the model also contribute in part to the noted underestimation of ϵ_N .

In light of the uncertainties in the photochemical mechanisms, prognostic model forecasts of meteorological fields and emissions, the overall performance of the model system can be considered to be reasonable with NMB less than 30% in general. On the other hand, given the fact that the three mechanisms use different method to condense the organic chemistry and have different number of species, leading to difficulty for defining completely equivalent emissions as well as complicating comparisons of chemistry in the three mechanisms, it is not obviously possible to prove which one is “correct” for O₃ and its related precursor predictions. On the basis of this work, overall none of the mechanisms performs systematically better than the others. However, it is important and necessary that the older chemical mechanisms be revised periodically to be consistent with current scientific knowledge. The CB05 mechanism has more detailed treatment of both inorganic and organic reactions and more number of species according to the state-of-the-science than CB4.

Acknowledgements

The authors would like to thank Drs. S.T. Rao, D. Luecken and two anonymous reviewers for the constructive and very helpful comments that led to a substantial

strengthening of the content of the paper. We thank Jeff McQueen, Pius Lee, and Marina Tsidulko for collaboration and critical assistance in performing the forecast simulations. We are grateful to the 2004 ICARTT investigators for making their measurement data available. The AIRMAP data were obtained from the University of New Hampshire's AIRMAP Observing Stations that are supported through NOAA's Office of Oceanic and Atmospheric Research. The United States Environmental Protection Agency through its Office of Research and Development funded and managed the research described here. It has been subjected to Agency's administrative review and approved for publication.

References

- Arnold, J.R., Dennis, R.L., and Tonnesen, G.S.,: Diagnostic evaluation of numerical air quality models with specialized ambient observations: testing the Community Multiscale Air Quality modeling system (CMAQ) at selected SOS 95 ground sites. *Atmos. Environ.*, 37, 1185-1198, 2003.
- Byun, D.W., and Schere, K.L.,: Review of the governing equations, computational algorithms, and other components of the models-3 Community Multi-scale Air Quality (CMAQ) modeling system, *Applied Mechanics Reviews*, 59, 51-77, 2006.
- Carter, W.P.L.,: Implementation of the SAPRC-99 chemical mechanism into the models-3 framework. Report to the United States Environmental Protection Agency, 2000. (<http://www.engr.ucr.edu/~carter/pubs/s99mod3.pdf>).
- Dennis, R.L., Byun, D.W., Novak, J.H., Gallupi, K.J., Coats, C.J., and Vouk, M.A.,: The next generation of integrated air quality modeling: EPA's Models-3. *Atmos. Environ.*, 30 (12), 1925-1938, 1996.
- Dodge, M. C.,: A comparison of photochemical oxidant mechanisms, *J. Geophys. Res.*, 94, 5121-5136, 1989.
- Dunker, A.M., Kumar, S., and Berzins, P.H.,: A comparison of chemical mechanisms used in atmospheric models, *Atmos. Environ.*, 18, 311-321, 1984.

- Faraji, M., Kimura, Y., McDonald-Buller, E., Allen, D., Comparison of the Carbon Bond and SAPRC photochemical mechanisms under conditions relevant to southeast Texas. *Atmos. Environ.*, 42, 5821–5836, doi:10.1016/j.atmosenv.2007.07.048, 2008
- Gery, M.W., Whitten, G.Z., Killus, J.P., Dodge, M.C.,: A photochemical kinetics mechanism for urban and regional scale computer modeling. *Journal of Geophysical Research* 94 (D10), 12925–12956, 1989.
- Guenther, A., Geron, C., Pierce, T., Lamb, B., Harley, P., and Fall, R.,: Natural emissions of non-methane volatile organic compounds; carbon monoxide, and oxides of nitrogen from North America, *Atmos. Environ.*, 34 (12–14), 2205–2230, 2000.
- Guenther, A., T. Karl, P. Harley, C. Wiedinmyer, P. Palmer, and C. Geron, Estimates of global terrestrial isoprene emissions using MEGAN (Model of Emissions of Gases and Aerosols from Nature), *Atmos. Chem Phys.*, 6, 3181–3210, 2006.
- Gross, A., Stockwell, W.,: Comparison of the EMEP, RADM2 and RACM mechanisms. *Journal of Atmospheric Chemistry* 44, 151–170, 2003.
- Henderson, B. Pinder, W. Goliff, W. Stockwell, A. Fahr, G. Sarwar, B. Hutzell, R. Mathur, W. Vizuete, R. Cohen, 2009. The role of chemistry in under-predictions of NO₂ in the upper troposphere, AGU Fall Meeting, 14–18 December, 2009, San Francisco, California, USA.
- Jenkin, M.E., Saunders, S.M., and Pilling, M.J.,: The tropospheric degradation of volatile organic compounds: A protocol for mechanism development, *Atmos. Environ.*, 31, 81–104, 1997.
- Jimenez, P., Baldasano, J.M., Dabdub, D.,: Comparison of photochemical mechanisms for air quality modeling. *Atmos. Environ.*, 37, 4179–4194, 2003.
- Kuhn, M., Builtjes, P.J.H., Poppe, D., Simpson, D., Stockwell, W.R., Andersson-Skold, Y., Baart, A., Das, M., Fiedler, F., Hov, O., Kirchner, F., Makar, P.A., Milford, J.B., Roemer, M.G.M., Ruhnke, R., Strand, A., Vogel, B., Vogel, H.,: Intercomparison of the gas-phase chemistry in several chemistry and transport models. *Atmos. Environ.*, 32, 693–709, 1998.

- Lee, M., Heikes, B.G., O'Sullivan, D.W.: Hydrogen peroxide and organic hydroperoxide in the troposphere: a review. *Atmos. Environ.*, 34, 3475–3494, 2000.
- Luecken, D.J., Tonnesen, G.S., Sickles, J.E.: Differences in NO_y speciation predicted by three photochemical mechanisms. *Atmos. Environ.*, 33, 1073–1084, 1999.
- Luecken, D.J., Phillips, S., Sarwar, G., Jang, C.: Effects of using the CB05 vs. SAPRC99 vs. CB4 chemical mechanism on model predictions: Ozone and gas-phase photochemical precursor concentrations. *Atmos. Environ.*, 42, 5805–5820, 2008.
- Mao, H., and Talbot, R.: O₃ and CO in New England: Temporal variations and relationships, *J. Geophys. Res.*, 109(D21304), doi:10.1029/2004JD004913, 2004.
- Mathur, R., Young, J.O., Schere, K.L., Gipson, G.L.: A comparison of numerical techniques for solution of atmospheric kinetic equations, *Atmos. Environ.*, 32, 1535–1553, 1998.
- Mathur, R.: Estimating the Impact of the 2004 Alaskan Forest Fires on Episodic Particulate Matter Pollution over the Eastern United States through Assimilation of Satellite Derived Aerosol Optical Depth in a Regional Air Quality Model, *J. Geophys. Res.*, 113, D17302, doi:10.1029/2007JD009767, 2008.
- McRae, G.J., Goodin, W.R., Seinfeld, J.H., Numerical solution of atmospheric diffusion equation for chemically reactive flows. *J. Comput. Physics.*, 45, 1–42, 1982
- Pouliot, G.A.: The emissions processing system for the Eta/CMAQ air quality forecast system, Proc. 7th Conf. on Atmospheric Chemistry, The 85th AMS Annual Meeting, Paper 4.5, Amer. Meteor. Soc., San Diego, CA, 2005.
- Ridley, B. A., Pickering, K.E., and Dye, J.E.: Comments on the parameterization of lightning-produced NO in global chemistry-transport models, *Atmos. Environ.*, 39, 6184–6187, 2005
- Rogers, E., Black, T., Deaven, D., DiMego, G., Zhao, Q., Baldwin, M., Junker, N., and Lin, Y.: Changes to the operational “early” Eta Analysis/Forecast System at the National Centers for Environmental Prediction. *Wea. Forecasting*, 11, 391–413, 1996.

- Russell, A., Dennis, R.: NARSTO critical review of photochemical models and modeling. *Atmos. Environ.*, 34, 2283–2324, 2000.
- Singh, H.B., Salas, L., Herlth, D., etc.: Reactive nitrogen distribution and partitioning in the North American troposphere and lowermost stratosphere. *J. Geophys. Res.*, 112, D12S04, doi:10.1029/2006JD007664, 2007.
- Stockwell, W.R.: A homogeneous gas phase mechanism for use in a regional acid deposition model. *Atmos. Environ.*, 20, 1615–1632, 1986.
- Yarwood, G., Rao, S., Yocke, M., Whitten, G.Z.: Updates to the Carbon Bond chemical mechanism: CB05. Final Report to the US EPA, RT-0400675, December 8, 2005 (http://www.camx.com/publ/pdfs/CB05_Final_Report_120805.pdf), 2005
- Yu, S.C., Eder, B., Dennis, R., Chu, S-H., and Schwartz, S.: New unbiased symmetric metrics for evaluation of air quality models. *Atmospheric Science Letter*, 7, 26-34, 2006.
- Yu, S.C., Mathur, R., Kang, D., Schere, K., Pleim, J., and Otte, T.L.: A detailed evaluation of the Eta-CMAQ forecast model performance for O₃, its related precursors, and meteorological parameters during the 2004 ICARTT study, *J. Geophys. Res.*, 112, D12S14, doi:10.1029/2006JD007715, 2007.

Table 1. Comparison of the reaction rates of inorganic species at 298 K and 1 atm (sec^{-1} for first order reactions, $\text{cm}^3 \text{molecule}^{-1} \text{sec}^{-1}$ for second-order, $\text{cm}^6 \text{molecule}^{-2} \text{sec}^{-1}$ for third-order reactions) in CB4, CB05 and SAPRC-99. Details on reaction rates and species can be found in Gery et al. (1989), Yarwood et al. (2005) and Carter (2000) for CB4, CB05 and SAPRC-99, respectively.

Reaction	CB4	CB05	SAPRC-99	Comments
NO₃ and O₃ chemistry				
NO ₂ +hν→NO+O	photolysis	photolysis	photolysis	
O ₃ +hν→O+O ₂	photolysis	photolysis	photolysis	
O ₃ +hν→OSD+O ₂	photolysis	photolysis	photolysis	
HONO+hν→NO+OH	photolysis	photolysis	photolysis	
HONO+hν→NO ₂ +HO ₂			photolysis	Not in CB4, CB05
O+O ₂ +M→O ₃ +M	5.57E-34	6.11E-34	5.79E-34	
O+NO→NO ₂	1.66E-12	1.66E-12	2.48E-12	
O+NO ₂ →NO+O ₂	9.30E-12	1.02E-11	9.72E-12	
O+O ₃ →2O ₂			7.96E-15	Not in CB4, CB05
O1D+H ₂ O→2OH	2.20E-10	2.20E-10	2.20E-10	
O1D+M→O+M	2.58E-11	2.96E-11	2.87E-11	
O ₃ +OH→HO ₂ +O ₂	6.83E-14	7.25E-14	6.63E-14	
O ₃ +HO ₂ →OH+2O ₂	2.00E-15	1.93E-15		Not in SAPRC-99
NO+NO+O ₂ →2NO ₂	1.95E-38	1.96E-38	1.95E-38	
NO+NO ₂ +H ₂ O→2HONO	4.40E-40	5.00E-40		Not in SAPRC-99
NO+O ₃ →NO ₂ +O ₂	1.81E-14	1.95E-14	1.81E-14	
NO+OH+M→HONO+M	6.70E-12	7.41E-12	7.41E-12	
NO+HO ₂ →NO ₂ +OH	8.28E-12	8.10E-12	8.41E-12	
NO ₂ +NO ₃ →NO+NO ₂ +O ₂	4.03E-16	6.56E-16	6.56E-16	
NO ₂ +HO ₂ +M→HNO ₄ +M	1.48E-12	1.38E-12	1.38E-12	
HONO+OH→NO ₂ +H ₂ O	6.60E-12	4.86E-12	6.46E-12	
HONO+HONO→NO+NO ₂	1.00E-20	1.00E-20		Not in SAPRC-99
HNO ₄ +M→NO ₂ +HO ₂ +M			7.55E-02	Not in CB4, CB05
HNO ₄ +OH→NO ₂ +O ₂ +H ₂ O			5.02E-12	Not in CB4, CB05
SO ₂ +OH→H ₂ SO ₄ +HO ₂	8.89E-13	8.89E-13	9.77E-13	
CO+OH→HO ₂ +CO ₂	2.40E-13	2.41E-13	2.09E-13	
NO₃ and HNO₃ chemistry				
NO ₃ +hν→NO+O ₂		photolysis	photolysis	Not in CB4
NO ₃ +hν→NO ₂ +O	photolysis	photolysis	photolysis	
HNO ₃ +hν→NO ₂ +OH		photolysis	photolysis	Not in CB4
HNO ₄ +hν→0.61HO ₂ +0.61NO ₂ +0.39OH+0.39NO ₃			photolysis	Not in CB4, CB05
O+NO ₂ +M→NO ₃ +M	1.58E-12	3.28E-12	1.82E-12	
NO ₂ +O ₃ →NO ₃ +O ₂	3.23E-17	3.23E-17	3.52E-17	
NO ₂ +OH→HNO ₃	1.15E-11	1.05E-11	8.98E-12	
HNO ₃ +OH→NO ₃ +H ₂ O	1.47E-13	1.54E-13	1.47E-13	
NO ₃ +OH→NO ₂ +HO ₂		2.20E-11	2.00E-11	Not in CB4
NO ₃ +HO ₂ →HNO ₃ +O ₂		3.50E-12		Not in CB4, SAPRC-99
NO ₃ +HO ₂ →0.8NO ₂ +0.2HNO ₃ +0.8OH+O ₂			4.00E-12	Not in CB4, CB05
NO ₃ +NO ₃ →2NO ₂ +O ₂		2.28E-16	2.28E-16	Not in CB4
NO ₃ +NO→2NO ₂	3.01E-11	2.65E-11	2.60E-11	
NO ₃ +NO ₂ +M→N ₂ O ₅ +M	1.26E-12	1.18E-12	1.54E-12	
N ₂ O ₅ →NO ₂ +NO ₃	4.36E-02	5.28E-02	5.28E-02	
N ₂ O ₅ +H ₂ O→2HNO ₃	0.00E+00	0.00E+00	0.00E+00	
HO₂ and H₂O₂ chemistry				
H ₂ O ₂ +hν→2OH	photolysis	photolysis	photolysis	
HO ₂ +OH→H ₂ O+O ₂		1.11E-10	1.11E-10	Not in CB4
HO ₂ +HO ₂ →H ₂ O ₂	2.80E-12	1.72E-12	1.64E-12	
HO ₂ +HO ₂ +H ₂ O→H ₂ O ₂ +O ₂ +H ₂ O	6.24E-30	3.87E-30	3.78E-30	
H ₂ O ₂ +OH→HO ₂ +H ₂ O	1.66E-12	1.70E-12	1.70E-12	
OH+H ₂ →HO ₂		6.69E-15	6.70E-15	Not in CB4

Table 2. The same as Table 1 but for organic species

Reactions	CB4	CB05	SAPRC-99	Comments
Formaldehyde				
HCHO + OH → HO2 + CO	1.00E-11	9.00E-12	9.20E-12	Formaldehyde
HCHO → 2HO2 + CO	photolysis	photolysis	photolysis	
HCHO → CO	photolysis	photolysis	photolysis	
HCHO + O → OH + HO2 + CO	1.65E-13	1.58E-13		
HCHO + NO3 → HNO3 + HO2 + CO	6.30E-16	5.80E-16	5.73E-16	
HCHO + HO2 → HCO3		7.90E-14	7.90E-14	
HCO3 → HCHO + HO2		1.51E+02	1.51E+02	
HCO3 + NO → HCOOH + NO2 + HO2		5.60E-12	7.29E-12	
HCO3 + HO2 → MEPX		1.26E-11		
HCOOH + OH → HO2		4.00E-13	4.50E-13	Formic acid
MEO2 + NO → HCHO + HO2 + NO2		7.66E-12	7.29E-12	Methylperoxy radical
MEO2 + HO2 → MEPX		5.08E-12	5.21E-12	
MEO2 + MEO2 → 1.37HCHO + 0.74HO2 + 0.63MEOH		3.52E-13		
MEOH + OH → HCHO + HO2		9.12E-13	9.14E-13	Methanol
MEPX → HCHO + HO2 + OH		photolysis	photolysis	Methylhydroperoxide
MEPX + OH → 0.7MEO2 + 0.3XO2 + 0.3HO2		7.43E-12		
MEO2 + MEO2 → MEOH + HCHO			2.65E-13	Methylperoxy radical
MEO2 + MEO2 → 2HCHO + 2HO2			1.07E-13	
MEO2 + NO3 → HCHO + HO2 + NO2			1.30E-12	
MEPX + HO → 0.35HCHO + 0.35HO + 0.65MEO2			5.49E-12	Methylhydroperoxide
Alkene reactions				
OLE + O → 0.63ALD2 + 0.38HO2 + 0.28XO2 + 0.3CO + 0.2HCHO + 0.02XO2N + 0.22PAR + 0.2OH	4.05E-12			Terminal Olefin
OLE + O → 0.2ALD2 + 0.3ALDX + 0.3HO2 + 0.2XO2 + 0.2CO + 0.2HCHO + 0.01XO2N + 0.2PAR + 0.1OH		3.91E-12		
OLE + OH → HCHO + ALD2 + XO2 + HO2 - PAR	2.82E-11			
OLE + OH → 0.8ALD2 + 0.33ALDX + 0.62ALDX + 0.8XO2 + 0.95HO2 - 0.7PAR		3.20E-11		
OLE + O3 → 0.5ALD2 + 0.74HCHO + 0.33CO + 0.44HO2 + 0.22XO2 + 0.1OH + 0.2HCOOH + 0.2AACD - PAR	1.20E-17			
OLE + O3 → 0.18ALD2 + 0.74HCHO + 0.32ALDX + 0.22XO2 + 0.1OH + 0.33CO + 0.44HO2 - 1.0PAR		1.11E-17		
OLE + NO3 → 0.91XO2 + 0.09XO2N + HCHO + ALD2 - PAR + NO2	7.70E-15			
NO3 + OLE → NO2 + HCHO + 0.91XO2 + 0.09XO2N + 0.56ALDX + 0.35ALD2 - 1PAR		4.98E-16		
OLE1 + HO → 0.91RO2_R + 0.09RO2_N + 0.205R2O2 + 0.732HCHO + 0.294ALD2 + 0.497RCHO + 0.005ACET + 0.119PROD2			3.23E-11	Alkene 1
OLE1 + O3 → 0.155HO + 0.056HO2 + 0.022RO2_R + 0.001RO2_N + 0.076MEO2 + 0.345CO + 0.5HCHO + 0.154ALD2 + 0.363RCHO + 0.001ACET + 0.215PROD2 + 0.185HCOOH + 0.05CCO_OH + 0.119RCO_OH			1.07E-17	
OLE1 + NO3 → 0.824RO2_R + 0.176RO2_N + 0.488R2O2 + 0.009ALD2 + 0.037RCHO + 0.024ACET + 0.511NTR			1.26E-14	
OLE1 + O → 0.45RCHO + 0.437MEK + 0.113PROD2			4.88E-12	
OLE2 + HO → 0.918RO2_R + 0.082RO2_N + 0.001R2O2 + 0.244HCHO + 0.732ALD2 + 0.511RCHO + 0.127ACET + 0.072MEK + 0.061BALD + 0.025METHACRO + 0.025ISOPROD + OLE2AER			6.31E-11	Alkene 2
OLE2 + O3 → 0.378HO + 0.003HO2 + 0.033RO2_R + 0.002RO2_N + 0.137R2O2 + 0.197MEO2 + 0.137C2O3 + 0.006RCO_O2 + 0.265CO + 0.269HCHO + 0.456ALD2 + 0.305RCHO + 0.045ACET + 0.026MEK + 0.006PROD2 + 0.042BALD + 0.026METHACRO + 0.073HCOOH + 0.129CCO_OH + 0.303RCO_OH + OLE2AER			1.07E-16	
OLE2 + NO3 → 0.391NO2 + 0.442RO2_R + 0.136RO2_N + 0.711R2O2 + 0.03MEO2 + 0.079HCHO + 0.507ALD2 + 0.151RCHO + 0.102ACET + 0.001MEK + 0.015BALD + 0.048MVK + 0.321NTR + OLE2AER			7.26E-13	
OLE2 + O → 0.013HO2 + 0.012RO2_R + 0.001RO2_N + 0.012CO + 0.069RCHO + 0.659MEK + 0.259PROD2 + 0.012METHACRO			2.09E-11	
ETH + O → HCHO + 0.7XO2 + CO + 1.7HO2 + 0.3OH	7.01E-13	7.29E-13		Ethene
ETH + O → 0.5HO2 + 0.2RO2_R + 0.3MEO2 + 0.491CO + 0.191HCHO + 0.25ALD2 + 0.009GLY			7.29E-13	
ETH + OH → XO2 + 1.56HCHO + HO2 + 0.22ALD2	7.94E-12	8.15E-12		
ETH + OH → RO2_R + 1.61HCHO + 0.195ALD2			8.52E-12	
ETH + O3 → HCHO + 0.42CO + 0.12HO2 + 0.4HCOOH	1.89E-18			
ETH + O3 → HCHO + 0.63CO + 0.13HO2 + 0.13OH + 0.37HCOOH		1.76E-18		
ETH + O3 → 0.12HO + 0.12HO2 + 0.5CO + HCHO + 0.37HCOOH			1.59E-18	
ETH + NO3 → NO2 + XO2 + 2HCHO		2.10E-16		
ETH + NO3 → RO2_R + RCHO			2.05E-16	
IOLE + O → 1.24ALD2 + 0.66ALDX + 0.1HO2 + 0.1XO2 + 0.1CO + 0.1PAR		2.30E-11		Internal olefin
IOLE + OH → 1.300ALD2 + 0.700ALDX + HO2 + XO2		6.33E-11		
IOLE + O3 → 0.65ALD2 + 0.35ALDX + 0.25HCHO + 0.25CO + 0.5O + 0.5OH + 0.5HO2		2.09E-16		
IOLE + NO3 → 1.180ALD2 + 0.640ALDX + HO2 + NO2		3.88E-13		
METHACRO + HO → 0.5RO2_R + 0.416CO + 0.084HCHO + 0.416MEK + 0.084MGLY + 0.5MA_RCO3			3.36E-11	Methacrolein

Table 2. Continued

Reactions	CB4	CB05	SAPRC-99	Comments
METHACRO + O3→ 0.008HO2 + 0.1RO2_R + 0.208HO + 0.1RCO_O2 + 0.45CO + 0.2HCHO + 0.9MGly + 0.333HCOOH			1.13E-18	
METHACRO + NO3→0.5HNO3 + 0.5RO2_R + 0.5CO + 0.5MA_RCO3			4.58E-15	
METHACRO + O3P→ RCHO			6.34E-12	
METHACRO→0.34HO2 + 0.33RO2_R + 0.33HO + 0.67C2O3 + 0.67CO + 0.67HCHO + 0.33MA_RCO3			photolysis	
MA_RCO3 + NO2→ MA_PAN			1.21E-11	Peroxyacyl radicals from methacrolein
MA_RCO3 + NO→ NO2 + HCHO + C2O3			2.80E-11	
MA_RCO3 + HO2→0.75RCO_OOH + 0.25RCO_OH + 0.25O3			1.41E-11	
MA_RCO3 + NO3→ NO2 + HCHO + C2O3			4.00E-12	
MA_RCO3 + MEO2 → RCO_OH + HCHO			9.64E-12	
MA_RCO3 + RO2_R→ RCO_OH			7.50E-12	
MA_RCO3 + R2O2 → MA_RCO3			7.50E-12	
MA_RCO3 + RO2_N→ 2RCO_OH			7.50E-12	
MA_RCO3 + C2O3→ MEO2 + HCHO + C2O3			1.55E-11	
MA_RCO3 + RCO_O2→ HCHO + C2O3 + ALD2 + RO2_R			1.55E-11	
MA_RCO3 + BZCO_O2→ HCHO + C2O3 + BZ_O + R2O2			1.55E-11	
MA_RCO3 + MA_RCO3 → 2HCHO + 2C2O3			1.55E-11	
Isoprene reactions				
ISOP + O→ 0.75ISPD + 0.50HCHO + 0.25XO2 + 0.25HO2 + 0.25C2O3 + 0.25PAR	3.60E-11	3.60E-11		Isoprene
ISOP + O→ 0.01RO2_N + 0.24R2O2 + 0.25MEO2 + 0.24MA_RCO3 + 0.24HCHO + 0.75PROD2			3.60E-11	
ISOP + OH→ 0.912ISPD + 0.629HCHO + 0.991XO2 + 0.912HO2 + 0.088XO2N	9.97E-11	9.97E-11		
ISOP + HO→ 0.907RO2_R + 0.093RO2_N + 0.079R2O2 + 0.624HCHO + 0.23METHACRO + 0.32MVK + 0.357ISOPROD			9.83E-11	
ISOP + O3→0.65ISPD + 0.60HCHO + 0.20XO2 + 0.066HO2 + 0.266OH + 0.20C2O3 + 0.15ALD2 + 0.35PAR + 0.066CO	1.29E-17	1.29E-17		
ISOP + O3→0.266HO + 0.066RO2_R + 0.008RO2_N + 0.126R2O2 + 0.192MA_RCO3 + 0.275CO + 0.592HCHO + 0.1PROD2 + 0.39METHACRO + 0.16MVK + 0.204HCOOH + 0.15RCO_OH			1.29E-17	
ISOP + NO3→0.2ISPD + 0.8NTR + 1XO2 + 0.8HO2 + 0.2NO2 + 0.8ALD2 + 2.4PAR	6.74E-13	6.74E-13	6.74E-13	
ISOP + NO2→0.2ISPD + 0.8NTR + 1XO2 + 0.8HO2 + 0.2NO + 0.8ALD2 + 2.4PAR	1.49E-19	1.50E-19		
ISPD + OH→1.565PAR + 0.167HCHO + 0.713XO2 + 0.503HO2 + 0.334CO + 0.168MGly + 0.273ALD2 + 0.498C2O3	3.36E-11			Isoprene product
ISPD + OH→1.565PAR + 0.167HCHO + 0.713XO2 + 0.503HO2 + 0.334CO + 0.168MGly + 0.252ALD2 + 0.21C2O3 + 0.25CXO3 + 0.12ALDX		3.36E-11		
ISPD + OH→0.67RO2_R + 0.041RO2_N + 0.289MA_RCO3 + 0.336CO + 0.055HCHO + 0.129ALD2 + 0.013RCHO + 0.15MEK + 0.332PROD2 + 0.15GLY + 0.174MGly			6.19E-11	
ISPD + O3→ 0.114C2O3 + 0.15HCHO + 0.85MGly + 0.154HO2 + 0.268OH + 0.064XO2 + 0.02ALD2 + 0.36PAR + 0.225CO	7.11E-18	7.10E-18		
ISPD + O3→ 0.4HO2 + 0.048RO2_R + 0.048RCO_O2 + 0.285HO + 0.498CO + 0.125HCHO + 0.047ALD2 + 0.21MEK + 0.023GLY + 0.742MGly + 0.1HCOOH + 0.372RCO_OH			4.18E-18	
ISPD + NO3→0.357ALD2 + 0.282HCHO + 1.282PAR + 0.925HO2 + 0.643CO + 0.850NTR + 0.075C2O3 + 0.075XO2 + 0.075HNO3	1.00E-15			
ISPD + NO3→0.357ALDX + 0.282HCHO + 1.282PAR + 0.925HO2 + 0.643CO + 0.85NTR + 0.075CXO3 + 0.075XO2 + 0.15HNO3		1.00E-15		
ISPD + NO3→0.799RO2_R + 0.051RO2_N + 0.15MA_RCO3 + 0.572CO + 0.15HNO3 + 0.227HCHO + 0.218RCHO + 0.008MGly + 0.572NTR			1.00E-13	
ISPD→0.333CO + 0.067ALD2 + 0.900HCHO + 0.832PAR + 1.033HO2 + 0.700XO2 + 0.967C2O3	photolysis	photolysis		
ISPD→1.233HO2 + 0.467C2O3 + 0.3RCO_O2 + 1.233CO + 0.3HCHO + 0.467ALD2 + 0.233MEK			photolysis	
Terpene reactions				
TERP + O→ 0.150ALDX + 5.12PAR + TERPAER		3.60E-11		Terpenes
TRP1 + O→0.147RCHO + 0.853PROD2 + TRP1AER			3.27E-11	Terpenes
TERP + OH→ TERPAER + OH	8.26E-11			
TERP + OH→0.750HO2 + 1.250XO2 + 0.250XO2N + 0.280HCHO + 1.66 PAR + 0.470ALDX + TERPAER		6.77E-11	8.26E-11	
TERP + NO3→ TERPAER + NO3	6.58E-12			
TERP + NO3→ 0.47NO2 + 0.28HO2 + 1.03XO2 + 0.25XO2N + 0.47ALDX + 0.53NTR + TERPAER		6.66E-12		
TRP1 + NO3→ 0.474NO2 + 0.276RO2_R + 0.25RO2_N + 0.75R2O2 + 0.474RCHO + 0.276NTR + TRP1AER			6.58E-12	
TERP + O3→ TERPAER + O3	6.87E-17			
TERP + O3→0.57OH + 0.07HO2 + 0.76XO2 + 0.18XO2N + 0.24HCHO + 0.001CO + 7PAR + 0.21ALDX + 0.39CXO3 + TERPAER		7.63E-17		
TRP1 + O3→ 0.567HO + 0.033HO2 + 0.031RO2_R + 0.18RO2_N + 0.729R2O2 + 0.123C2O3 + 0.201RCO_O2 + 0.157CO + 0.235HCHO + 0.205RCHO + 0.13ACET + 0.276PROD2 + 0.001GLY + 0.031BACL + 0.103HCOOH + 0.189RCO_OH + TRP1AER			6.87E-17	

Table 2. Continued

Reactions	CB4	CB05	SAPRC-99	Comments
Higher molecular weight Aldehyde				
ALD2 + O → C2O3 + OH	4.39E-13	4.49E-13		Acetaldehyde
ALD2 + OH → C2O3	1.62E-11	1.39E-11	1.58E-11	
ALD2 + NO3 → C2O3 + HNO3	2.50E-15	2.38E-15	2.73E-15	
ALD2 → MEO2 + CO + HO2		photolysis	photolysis	
ALD2 → XO2 + 2HO2 + CO + HCHO	photolysis			
C2O3 + NO → NO2 + XO2 + HCHO + HO2	1.91E-11	2.00E-11	2.13E-11	Acetylperoxy radical
C2O3 + NO2 → PAN	9.41E-12	1.05E-11	1.05E-11	
C2O3 + C2O3 → 2XO2 + 2HCHO + 2HO2	2.50E-12		1.55E-11	
C2O3 + C2O3 → 2MEO2		1.55E-11		
C2O3 + HO2 → 0.79HCHO + 0.79XO2 + 0.79HO2 + 0.79OH + 0.21PACD	6.50E-12			
C2O3 + HO2 → 0.8PACD + 0.2AACD + 0.2O3		1.41E-11		
C2O3 + MEO2 → 0.9MEO2 + 0.9HO2 + HCHO + 0.1AACD		1.07E-11		
C2O3 + XO2 → 0.9MEO2 + 0.1AACD		1.60E-11		
C2O3 + MEO2 → CCO_OH + HCHO			9.64E-12	
C2O3 + HO2 → 0.75CCO_OOH + 0.25CCO_OH + 0.25O3			1.41E-11	
C2O3 + NO3 → MEO2 + NO2			4.00E-12	
C2O3 + RO2_R → CCO_OH			7.50E-12	
C2O3 + R2O2 → C2O3			7.50E-12	
C2O3 + RO2_N → CCO_OH + PROD2			7.50E-12	
PAN → C2O3 + NO2	4.23E-04	3.31E-04	5.21E-04	Peroxyl acyl nitrate
PAN → C2O3 + NO2		photolysis		
PAN2 → RCO_O2 + NO2			4.43E-04	PPN and other higher alky PAN analogues
MA_PAN → MA_RCO3 + NO2			3.55E-04	
PACD + OH → C2O3		7.83E-13		Peroxycarboxylic acid
PACD → MEO2 + OH		photolysis		
AACD + OH → MEO2		7.83E-13		Carboxylic acid
ALDX + O → CXO3 + OH		7.02E-13		Propionaldehyde and higher aldehydes
ALDX + OH → CXO3		1.99E-11		
ALDX + NO3 → CXO3 + HNO3		6.50E-15		
ALDX → MEO2 + CO + HO2		photolysis		
CXO3 + NO → ALD2 + NO2 + HO2 + XO2		2.10E-11		C3 and higher acylperoxy radical
CXO3 + NO2 → PANX		1.05E-11		
CXO3 + HO2 → 0.8PACD + 0.2AACD + 0.2O3		1.41E-11		
CXO3 + MEO2 → 0.9ALD2 + 0.9XO2 + HO2 + 0.1AACD + 0.1HCHO		1.07E-11		
CXO3 + XO2 → 0.9ALD2 + 0.1AACD		1.60E-11		
CXO3 + CXO3 → 2ALD2 + 2XO2 + 2HO2		1.55E-11		
CXO3 + C2O3 → MEO2 + XO2 + HO2 + ALD2		1.55E-11		
PANX → CXO3 + NO2		3.31E-04		C3 and higher peroxyacyl nitrates
PANX → CXO3 + NO2		photolysis		
PANX + OH → ALD2 + NO2		3.00E-13		
NTR + OH → HNO3 + HO2 + 0.33HCHO + 0.33ALD2 + 0.33ALDX - 0.66PAR		1.76E-13		Organic nitrate (RNO3)
NTR → NO2 + HO2 + 0.33HCHO + 0.33ALD2 + 0.33ALDX - 0.66PAR		photolysis		
NTR + HO → 0.338NO2 + 0.113HO2 + 0.376RO2_R + 0.173RO2_N + 0.596R2O2 + 0.01HCHO + 0.439ALD2 + 0.213RCHO + 0.006ACET + 0.177MEK + 0.048PROD2 + 0.31NTR			7.80E-12	
NTR → NO2 + 0.341HO2 + 0.564RO2_R + 0.095RO2_N + 0.152R2O2 + 0.134HCHO + 0.431ALD2 + 0.147RCHO + 0.02ACET + 0.243MEK + 0.435PROD2			photolysis	
ROOH + OH → XO2 + 0.5ALD2 + 0.5ALDX		5.69E-12		Higher organic peroxide
ROOH + HO → RCHO + 0.34RO2_R + 0.66HO			1.10E-11	
ROOH → OH + HO2 + 0.5ALD2 + 0.5ALDX		photolysis		
ETOH + OH → HO2 + 0.9ALD2 + 0.05ALDX + 0.1HCHO + 0.1XO2		3.19E-12		Ethanol
ROOH → RCHO + HO2 + HO			photolysis	Lumped C3+ aldehydes
RCHO + HO → 0.034RO2_R + 0.001RO2_N + 0.965RCO_O2 + 0.034CO + 0.034ALD2			2.00E-11	
RCHO + NO3 → HNO3 + RCO_O2			3.67E-15	
RCHO → ALD2 + RO2_R + CO + HO2			photolysis	
CCO_OH + HO → 0.13RO2_R + 0.87MEO2 + 0.13MGly			8.00E-13	Peroxy acetic acid
RCO_OH + HO → RO2_R + 0.605ALD2 + 0.21RCHO + 0.185BACL			1.16E-12	Higher organic acids
Alkane reactions				
CH4 + OH → XO2 + HCHO + HO2	7.73E-15			Methane
CH4 + OH → MEO2		6.34E-15	6.37E-15	
ETHA + OH → 0.991ALD2 + 0.991XO2 + 0.009XO2N + HO2		2.40E-13		Ethane
PAR + OH → 0.87XO2 + 0.13XO2N + 0.11HO2 + 0.11ALD2 + 0.76ROR - 0.11PAR	8.10E-13			Paraffin carbon bond
PAR + OH → 0.87XO2 + 0.13XO2N + 0.11HO2 + 0.06ALD2 - 0.11PAR + 0.76ROR + 0.05ALDX		8.10E-13		
ROR → 1.1ALD2 + 0.96XO2 + 0.94HO2 - 2.10PAR + 0.04XO2N + 0.02ROR	2.19E+03			Secondary alkoxy radical

Table 2. Continued

Reactions	CB4	CB05	SAPRC-99	Comments
ROR→0.96XO2+0.6ALD2+0.94HO2-2.1PAR+0.04XO2N+0.02ROR+0.5ALDX		2.19E+03		
ROR→HO2	1.60E+03	1.60E+03		
ROR+NO2→NTR	1.50E-11	1.50E-11		
ALK1+HO→RO2_R+ALD2			2.54E-13	Alkane 1
ALK2+HO→0.246HO+0.121HO2+0.612RO2_R+0.021RO2_N+0.16CO+0.039HCHO+0.155RCHO+0.417ACET+0.248GLY+0.121HCOOH			1.04E-12	Alkane 2
ALK3+HO→0.695RO2_R+0.07RO2_N+0.559R2O2+0.236TBU_O+0.026HCHO+0.445ALD2+0.122RCHO+0.024ACET+0.332MEK			2.38E-12	Alkane 3
ALK4+HO→0.835RO2_R+0.143RO2_N+0.936R2O2+0.011MEO2+0.011C2O3+0.002CO+0.024HCHO+0.455ALD2+0.244RCHO+0.452ACET+0.11MEK+0.125PROD2			4.38E-12	Alkane 4
ALK5+HO→0.653RO2_R+0.347RO2_N+0.948R2O2+0.026HCHO+0.099ALD2+0.204RCHO+0.072ACET+0.089MEK+0.417PROD2+ALK5AER			9.32E-12	Alkane 5
Aromatic reactions				
TOL+OH→0.08XO2+0.36CRES+0.44HO2+0.56TO2+TOLAER	6.19E-12	5.92E-12		Toluene
ARO1+OH→0.224HO2+0.765RO2_R+0.011RO2_N+0.055PROD2+0.118GLY+0.119MGLY+0.017PHEN+0.207CRES+0.059BALD+0.491DCB1+0.108DCB2+0.051DCB3+ARO1AER			5.96E-12	Aromatic 1
TO2+NO→0.9NO2+0.9HO2+0.9OPEN+0.1NTR	8.10E-12	8.10E-12		Toluene-hydroxyl radical adduct
TO2→CRES+HO2	4.20E+00	4.20E+00		
ARO2+HO→0.187HO2+0.804RO2_R+0.009RO2_N+0.097GLY+0.287MGLY+0.087BACL+0.187CRES+0.05BALD+0.561DCB1+0.099DCB2+0.093DCB3+ARO2AER			2.64E-11	Aromatic 2
CRES+OH→0.4CRO+0.6XO2+0.6HO2+0.3OPEN+CSLAER	4.10E-11	4.10E-11		Cresols
CRES+OH→0.24BZ_O+0.76RO2_R+0.23MGLY+CRESAER			4.20E-11	
CRES+NO3→CRO+HNO3+CSLAER	2.20E-11	2.20E-11		
CRES+NO3→HNO3+BZ_O+CRESAER			1.37E-11	
CRO+NO2→NTR	1.40E-11	1.40E-11		
CRO+HO2→CRES		5.50E-12		Methylphenoxy radical
XYL+OH→0.7HO2+0.5XO2+0.2CRES+0.8MGLY+1.1PAR+0.3TO2+XYLAER	2.51E-11	2.51E-11		Xylene
OPEN+OH→XO2+2CO+2HO2+C2O3+HCHO	3.00E-11	3.00E-11		Aromatic ring opening product
OPEN→C2O3+HO2+CO	photolysis	photolysis		
OPEN+O3→0.03ALD2+0.62C2O3+0.7HCHO+0.03XO2+0.69CO+0.08OH+0.76HO2+0.2MGLY	1.01E-17	1.01E-17		
MGLY+OH→XO2+C2O3	1.70E-11	1.80E-11		Methylglyoxal
MGLY+HO→CO+C2O3			1.50E-11	
MGLY→C2O3+HO2+CO	photolysis	photolysis	photolysis	
MGLY+NO3→HNO3+CO+C2O3			2.42E-15	Glyoxal
GLY→2CO+2HO2			photolysis	
GLY→HCHO+CO			photolysis	
GLY+HO→0.63HO2+1.26CO+0.37RCO_O2			1.10E-11	
GLY+NO3→HNO3+0.63HO2+1.26CO+0.37RCO_O2			9.65E-16	
DCB1+HO→RCHO+RO2_R+CO			5.00E-11	Reactive aromatic fragmentation product 1
DCB1+O3→1.5HO2+0.5HO+1.5CO+GLY			2.00E-18	
DCB2+HO→R2O2+RCHO+C2O3			5.00E-11	Reactive aromatic fragmentation product 2
DCB2→RO2_R+0.5C2O3+0.5HO2+CO+R2O2+0.5GLY+0.5MGLY			photolysis	
DCB3+HO→R2O2+RCHO+C2O3			5.00E-11	Reactive aromatic fragmentation product 3
DCB3→RO2_R+0.5C2O3+0.5HO2+CO+R2O2+0.5GLY+0.5MGLY			photolysis	
PHEN+HO→0.24BZ_O+0.76RO2_R+0.23GLY			2.63E-11	Phenol
PHEN+NO3→HNO3+BZ_O			3.78E-12	
Ketone				
ACET+HO→HCHO+C2O3+R2O2			1.92E-13	Acetone
ACET→C2O3+MEO2			photolysis	
MEK+HO→0.37RO2_R+0.042RO2_N+0.616R2O2+0.492C2O3+0.096RCO_O2+0.115HCHO+0.482ALD2+0.37RCHO			1.18E-12	Ketones
MEK→C2O3+ALD2+RO2_R			photolysis	
MVK+HO→0.3RO2_R+0.025RO2_N+0.675R2O2+0.675C2O3+0.3HCHO+0.675RCHO+0.3MGLY			1.89E-11	Methyl vinyl ketones
MVK+O3→0.064HO2+0.05RO2_R+0.164HO+0.05RCO_O2+0.475CO+0.1HCHO+0.95MGLY+0.351HCOOH			4.58E-18	
MVK+O3P→0.45RCHO+0.55MEK			4.32E-12	
MVK→0.3MEO2+0.7CO+0.7PROD2+0.3MA_RCO3			photolysis	
PROD2+HO→0.379HO2+0.473RO2_R+0.07RO2_N+0.029C2O3+0.049RCO_O2+0.213HCHO+0.084ALD2+0.558RCHO+0.115MEK+0.329PROD2			1.50E-11	

Table 2. Continued

Reactions	CB4	CB05	SAPRC-99	Comments
PROD2 → 0.96RO2_R + 0.04RO2_N + 0.515R2O2 + 0.667C2O3 + 0.333RCO_O2 + 0.506HCHO + 0.246ALD2 + 0.71RCHO			photolysis	
other				
RO2_R + NO → NO2 + HO2			9.04E-12	Peroxy radical operator
RO2_R + HO2 → ROOH			1.49E-11	
RO2_R + NO3 → NO2 + HO2			2.30E-12	
RO2_R + MEO2 → HO2 + 0.75HCHO + 0.25MEOH			2.00E-13	
RO2_R + RO2_R → HO2			3.50E-14	
R2O2 + NO → NO2			9.04E-12	Peroxy radical operator
R2O2 + HO2 → HO2			1.49E-11	
R2O2 + NO3 → NO2			2.30E-12	
R2O2 + MEO2 → MEO2			2.00E-13	
R2O2 + RO2_R → RO2_R			3.50E-14	
R2O2 + R2O2 →			3.50E-14	
RO2_N + NO → NTR			9.04E-12	Peroxy radical operator
RO2_N + HO2 → ROOH			1.49E-11	
RO2_N + MEO2 → HO2 + 0.25MEOH + 0.5MEK + 0.5PROD2 + 0.75HCHO			2.30E-12	
RO2_N + NO3 → NO2 + HO2 + MEK			2.00E-13	
RO2_N + RO2_R → HO2 + 0.5MEK + 0.5PROD2			3.50E-14	
RO2_N + R2O2 → RO2_N			3.50E-14	
RO2_N + RO2_N → MEK + HO2 + PROD2			3.50E-14	
RCO_O2 + NO2 → PAN2			1.21E-11	Peroxy propionyl radicals
RCO_O2 + NO → NO2 + ALD2 + RO2_R			2.80E-11	
RCO_O2 + HO2 → 0.75RCO_OOH + 0.25RCO_OH + 0.25O3			1.41E-11	
RCO_O2 + NO3 → NO2 + ALD2 + RO2_R			4.00E-12	
RCO_O2 + MEO2 → RCO_OH + HCHO			9.64E-12	
RCO_O2 + RO2_R → RCO_OH			7.50E-12	
RCO_O2 + R2O2 → RCO_O2			7.50E-12	
RCO_O2 + RO2_N → RCO_OH + PROD2			7.50E-12	
RCO_O2 + C2O3 → MEO2 + ALD2 + RO2_R			1.55E-11	
RCO_O2 + RCO_O2 → 2ALD2 + 2RO2_R			1.55E-11	
BZCO_O2 + NO2 → PBZN			1.37E-11	Peroxy radicals from aromatic aldehyde
PBZN → BZCO_O2 + NO2			3.12E-04	
BZCO_O2 + NO → NO2 + BZ_O + R2O2			2.80E-11	
BZCO_O2 + HO2 → 0.75RCO_OOH + 0.25RCO_OH + 0.25O3			1.41E-11	
BZCO_O2 + NO3 → NO2 + BZ_O + R2O2			4.00E-12	
BZCO_O2 + MEO2 → RCO_OH + HCHO			9.64E-12	
BZCO_O2 + RO2_R → RCO_OH			7.50E-12	
BZCO_O2 + R2O2 → BZCO_O2			7.50E-12	
BZCO_O2 + RO2_N → RCO_OH + PROD2			7.50E-12	
BZCO_O2 + C2O3 → MEO2 + BZ_O + R2O2			1.55E-11	
BZCO_O2 + RCO_O2 → ALD2 + RO2_R + BZ_O + R2O2			1.55E-11	
BZCO_O2 + BZCO_O2 → 2BZ_O + 2R2O2			1.55E-11	
TBU_O + NO2 → NTR			2.40E-11	t-Butoxy radicals
TBU_O → ACET + MEO2			9.88E+02	
BZ_O + NO2 → NPHE			3.80E-11	Pheoxy radicals
BZ_O + HO2 → PHEN			1.49E-11	
BZ_O → PHEN			1.00E-03	
BZNO2_O + NO2 →			3.80E-11	Nitro-substituted phenoxy radicals
BZNO2_O + HO2 → NPHE			1.49E-11	
BZNO2_O → NPHE			1.00E-03	
NPHE + NO3 → HNO3 + BZNO2_O			3.78E-12	Nitrophenols
BACL → 2C2O3			photolysis	Biacetyl
BALD + HO → BZCO_O2			1.29E-11	Benzaldehyde
BALD →			photolysis	
BALD + NO3 → HNO3 + BZCO_O2			2.62E-15	

Table 3. Comparison of observations and models (CB4, CB05 and SAPRC-99) for different gaseous species (O₃, CO, PAN, NO_x, NO, NO₂, HNO₃, NO_y, ethylene, NO_z, and NO₂+O₃ on the basis of all P-3 and DC-8 aircraft measurements during the 2004 ICARTT (mean ± standard deviation, all units are ppbv except that PAN, isoprene, and terpenes units are pptv).

	Mean ± standard deviation				NMB (%)		
	Obs	CB4	CB05	SAPRC-99	CB4	CB05	SAPRC-99
P3							
O ₃	55.4±16.2	61.3±16.1	67.1±17.4	68.9±18.0	10.8	21.1	24.3
O ₃ +NO ₂	58.5±14.9	63.4±16.5	69.6±17.4	71.3±17.8	8.3	19.0	22.0
NO _z	2.7±1.4	5.4±2.4	5.5±2.5	4.3±2.1	101.2	108.0	63.1
PAN	348.1±176.7	1047.8±525.0	1054.0±544.1	768.9±445.0	201.0	202.8	120.9
NO _y	4.1±2.5	6.3±3.1	6.4±3.1	5.3±2.8	53.0	55.8	28.3
CO	139.3±36.0	124.8±33.2	129.6±33.2	121.2±35.5	-10.4	-6.9	-13.0
HNO ₃	1.8±1.8	1.6±1.6	1.4±1.4	1.5±1.5	-8.9	-19.9	-16.1
NO ₂	0.8±1.4	0.6±0.9	0.8±1.2	0.7±0.9	-22.5	-2.4	-19.3
NO	0.2±0.8	0.1±0.2	0.1±0.2	0.1±0.2	-56.2	-61.0	-56.8
NO _x	1.0±2.1	0.7±1.0	0.8±1.2	0.7±1.0	-32.8	-17.9	-30.4
SO ₂	1.7±2.7	1.5±2.0	1.6±2.0	1.7±2.0	-9.7	-2.9	-1.4
isoprene	69.7±100.4	65.5±140.9	73.5±145.7	63.8±138.5	-6.0	5.5	-8.4
terpenes	15.6±12.4	4.3±11.1	5.1±11.5	3.9±9.9	-72.2	-67.3	-74.9
DC-8							
O ₃	57.5±19.9	68.6±37.5	72.0±36.3	73.8±37.1	19.2	25.2	28.4
HNO ₃	0.8±0.8	0.9±0.9	0.8±0.8	0.9±0.9	13.5	0.7	4.7
HCHO	0.9±0.6	1.6±1.1	1.2±0.8	1.1±0.8	82.1	39.0	26.2
H ₂ O ₂	2.1±1.0	3.7±1.6	2.4±1.0	1.6±0.8	74.7	10.8	-25.5
CO	130.2±35.4	99.6±22.3	101.8±23.4	93.2±24.4	-23.5	-21.8	-28.4
NO ₂	0.5±1.3	0.3±0.8	0.3±0.7	0.4±0.7	-33.9	-35.0	-30.5
SO ₂	1.1±1.5	0.8±1.1	0.8±1.1	0.8±1.1	-26.1	-20.4	-21.5
NO	0.2±0.3	0.1±0.2	0.1±0.2	0.1±0.2	-58.6	-60.7	-55.3

Table 4. Comparison of observations and model predictions (CB4, CB05 and SAPRC-99) for different gaseous species (O₃, CO, PAN, NO, NO₂, NO_y, SO₂ and NO₂+O₃ along the ship tracks for different offshore flows during the 2004 ICARTT (mean ± standard deviation, all units are ppbv except that isoprene unit is pptv). Correlations between O₃ and NO_x for the NO_x limited conditions indicated by the observational data with [O₃]/[NO_x]>46 (aged air masses) (see text for explanation).

	Mean ± standard deviation				NMB (%)		
	Obs	CB4	CB05	SAPRC-99	CB4	CB05	SAPRC-99
Southwest/west offshore flows							
O ₃	44.6±18.9	56.9±23.0	62.7±25.2	65.6±27.6	27.6	40.6	47.1
O ₃ +NO ₂	48.1±17.6	60.5±19.5	66.0±22.1	69.0±24.7	25.6	37.1	43.4
isoprene	135.8±164.3	41.4±82.2	42.1±84.4	39.8±82.8	-69.5	-69.0	-70.7
CO	190.4±63.3	197.1±100.9	190.2±90.8	179.9±89.1	3.5	-0.1	-5.5
NO _y	6.7±7.4	10.6±10.8	10.2±10.0	8.8±9.8	58.1	52.6	31.8
NO ₂	3.5±4.5	3.6±7.4	3.4±6.9	3.5±7.0	5.3	-2.6	1.4
NO	1.0±2.5	1.1±4.5	0.8±3.9	0.8±3.9	9.7	-16.0	-15.4
PAN	0.7±0.6	1.1±0.7	1.2±0.8	0.8±0.6	60.4	72.4	24.3
SO ₂	1.1±1.2	2.1±2.2	2.3±2.1	2.3±2.1	97.5	113.3	117.1
East/north/northwest/south clean marine or continental flows							
O ₃	35.0±12.5	37.2±10.2	39.7±10.0	41.2±9.9	6.2	13.6	17.7
O ₃ +NO ₂	36.8±12.2	37.8±10.3	40.4±10.2	41.8±10.1	3.0	9.9	14.0
isoprene	81.3±95.8	71.4±141.1	81.7±148.6	78.8±151.9	-12.2	0.5	-3.0
CO	146.5±21.1	104.5±15.4	101.0±14.1	87.5±18.6	-28.6	-31.1	-40.3
NO _y	3.3±4.6	2.3±1.1	2.0±0.9	1.3±0.8	-31.3	-41.8	-62.6
NO ₂	1.6±2.0	0.6±0.8	0.4±0.6	0.5±0.6	-63.6	-72.5	-70.8
NO	1.5±10.8	0.03±0.07	0.02±0.05	0.02±0.05	-97.8	-98.5	-98.3
PAN	0.8±0.5	0.7±0.4	0.4±0.2	0.3±0.2	-11.7	-48.9	-65.6
SO ₂	0.6±0.9	0.39±0.39	0.37±0.36	0.38±0.37	-36.0	-38.8	-36.7
All data							
Obs (n=138):	[O ₃]=11.8[NO _x] +36.8, r = 0.591						
CB4 (n=138):	[O ₃]= 4.0[NO _x] +38.3, r = 0.805						
CB05 (n=138):	[O ₃]= 4.5[NO _x] +42.1, r = 0.798						
SAPRC-99 (n=138):	[O ₃]= 5.8[NO _x] +45.8, r = 0.786						

Table 5. Comparison of observations and model predictions (CB4, CB05 and SAPRC-99) for different gaseous species (O₃, CO, NO, NO_y, SO₂) at four AIRMAP sites during the 2004 ICARTT (mean ± standard deviation, all units are ppbv).

	Mean ± standard deviation				NMB (%)		
	Obs	CB4	CB05	SAPRC-99	CB4	CB05	SAPRC-99
Castle Springs (N=842)							
NO	0.14±0.2	0.05±0.07	0.04±0.05	0.04±0.05	-66.9	-73.7	-69.2
NO _y	2.2±1.5	3.4±2.5	3.1±2.4	2.4±2.0	55.9	41.9	9.8
O ₃	35.2±13.0	46.8±15.0	51.9±16.1	52.7±16.8	33.2	47.5	50.0
CO	189.8±45.5	112.1±31.2	113.1±31.5	105.0±32.7	-40.9	-40.4	-44.7
SO ₂	1.3±2.3	1.0±1.4	1.2±1.7	1.1±1.7	-21.2	-7.3	-13.2
Isle of Schoals (N=864)							
O ₃	36.8±17.1	52.4±16.9	57.7±19.8	58.9±21.9	42.2	56.6	59.9
CO	175.2±52.9	124.1±44.0	124.2±42.2	112.6±44.4	-29.1	-29.1	-35.7
NO	0.8±1.4	0.2±1.1	0.07±0.33	0.09±0.40	-74.5	-90.8	-88.1
Mount Washington (N=864)							
O ₃	46.6±12.7	49.3±14.3	53.3±15.5	54.7±16.8	5.7	14.3	17.4
NO	4.3±15.5	0.01±0.01	0.01±0.01	0.01±0.03	-99.7	-99.7	-99.6
CO	157.5±45.8	96.2±19.8	98.5±20.9	91.1±23.8	-38.9	-37.4	-42.2
NO _y	4.4±13.5	2.4±1.7	2.2±1.6	1.7±1.3	-44.4	-50.0	-61.0
SO ₂	0.9±1.6	0.4±0.5	0.5±0.7	0.5±0.7	-55.2	-44.8	-39.2
Thompson Farm (N=864)							
O ₃	28.2±18.7	43.9±17.7	49.7±18.2	51.4±19.5	55.3	76.1	82.0
NO	0.3±0.7	0.2±0.4	0.2±0.2	0.2±0.3	-28.6	-48.2	-47.5
CO	173.4±48.6	160.8±57.9	154.1±50.5	150.0±57.1	-7.3	-11.1	-13.6
NO _y	3.9±2.6	7.4±4.8	6.5±4.2	6.1±4.1	89.2	65.3	55.2
SO ₂	1.1±2.4	1.5±1.2	1.7±1.3	1.7±1.3	32.0	49.1	54.1

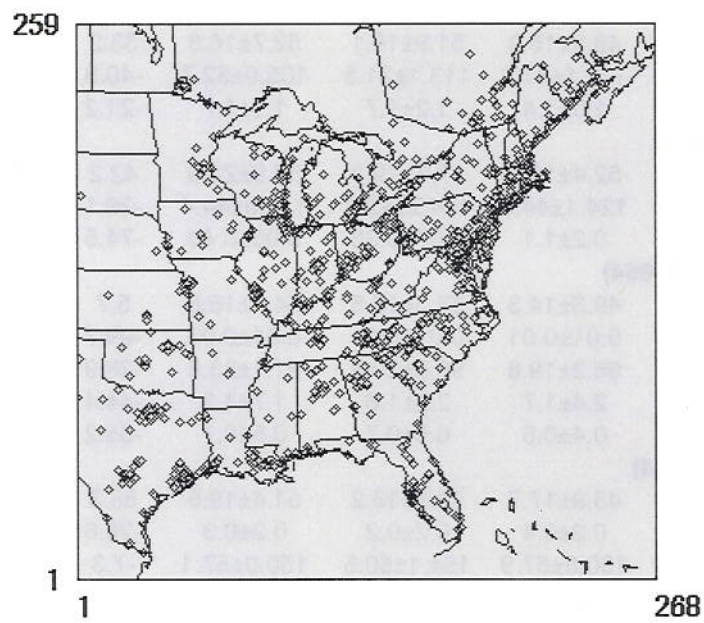
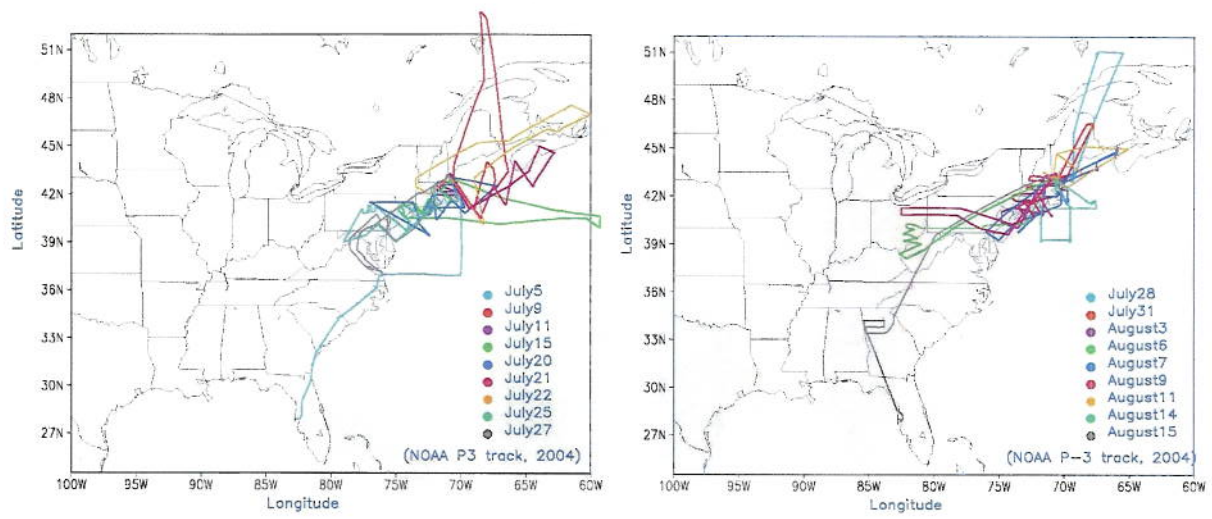
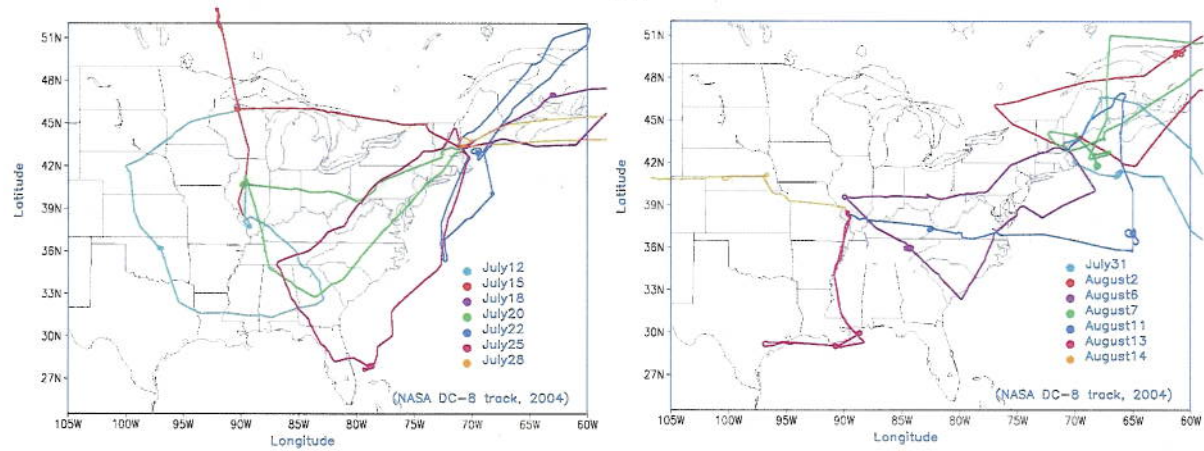


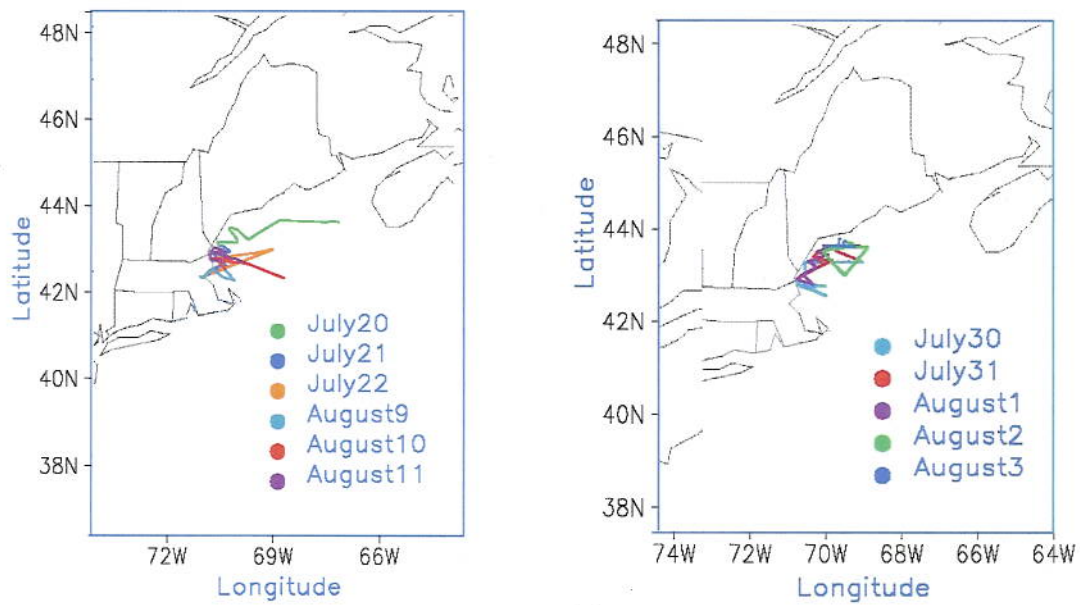
Figure 1. The model domain and locations of AIRNow monitoring sites.



(a)



(b)



(c)

Figure 2. Tracks of (a) P-3, (b) DC-8 and (c) ship tracks during the 2004 ICARTT period

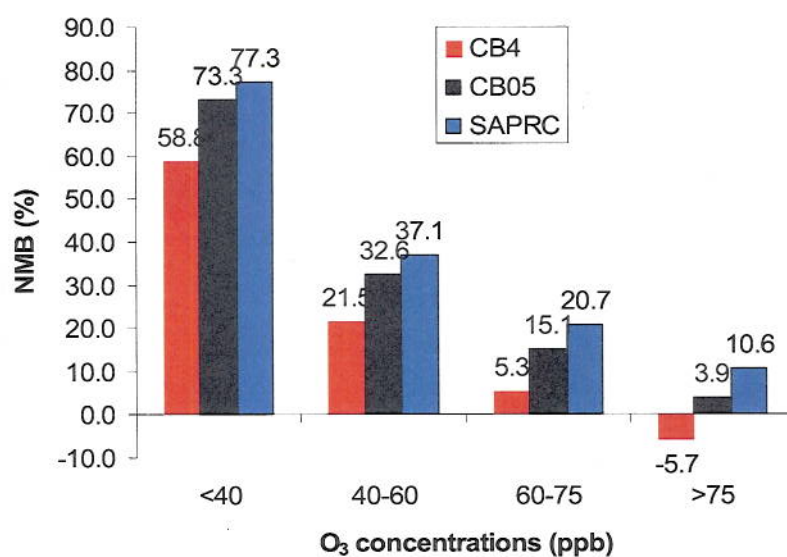


Figure 3. Comparison of the modeled (CB4, CB05 and SAPRC-99) and observed maximum 8-hour O₃ concentrations at the AIRNow monitoring sites: The NMB values of each model as a function of the observed maximum 8-hour O₃ concentration ranges during the period of 15 July and 18 August, 2004;

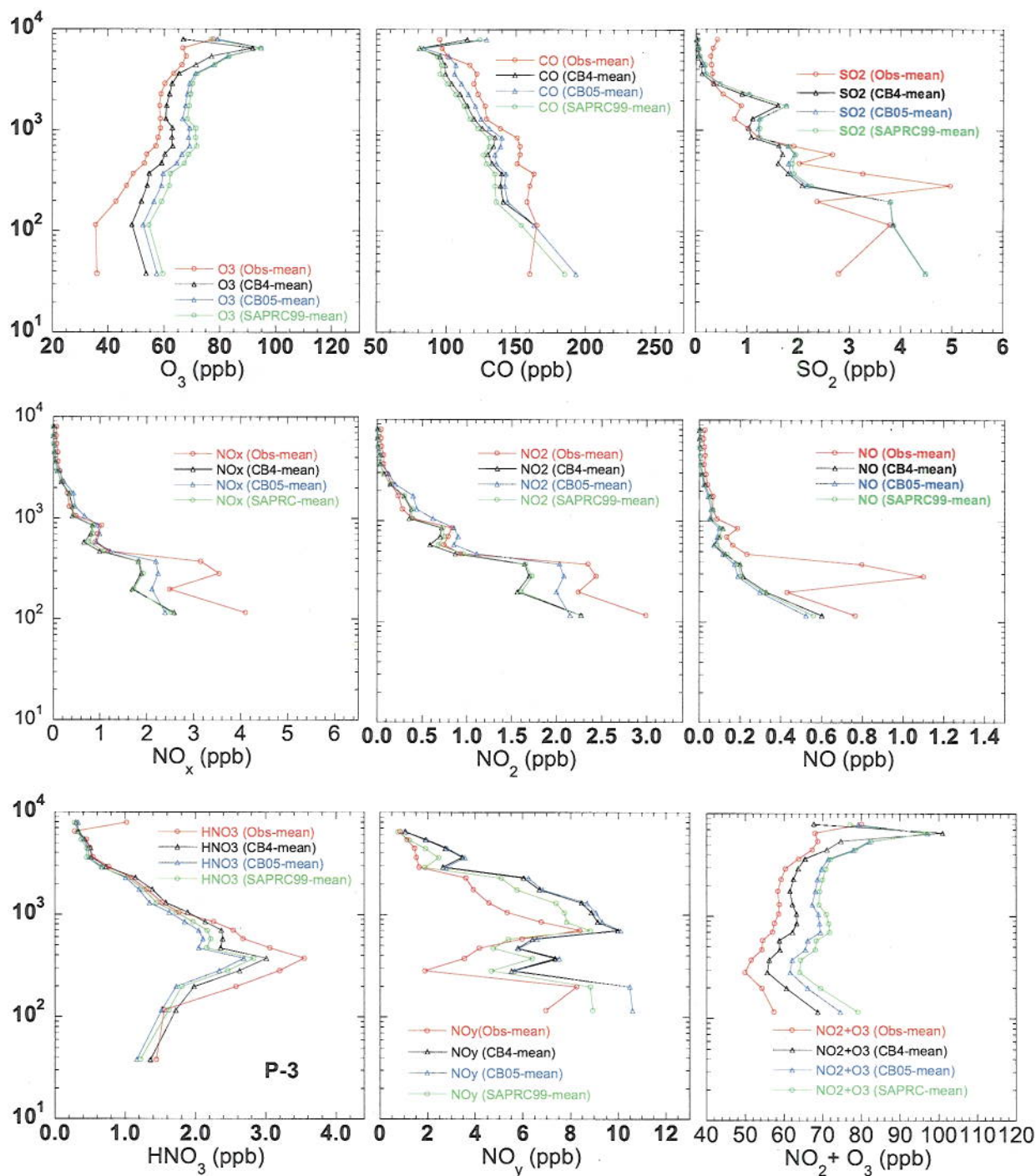


Figure 4. Comparison of means of vertical O_3 , CO , NO_x , NO , NO_2 , HNO_3 , NO_y and NO_2+O_3 for the P-3 observations and model predictions during 2004 ICARTT period.

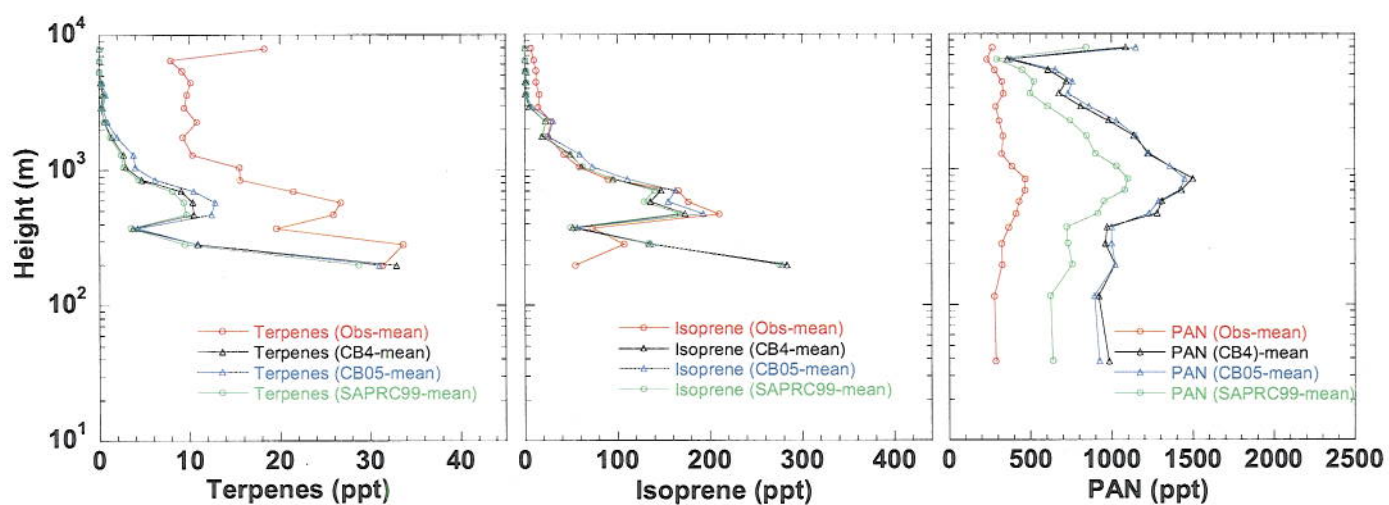


Figure 5. Comparison of means of vertical terpenes, isoprene and PAN for the P-3 observations and model predictions during 2004 ICARTT period.

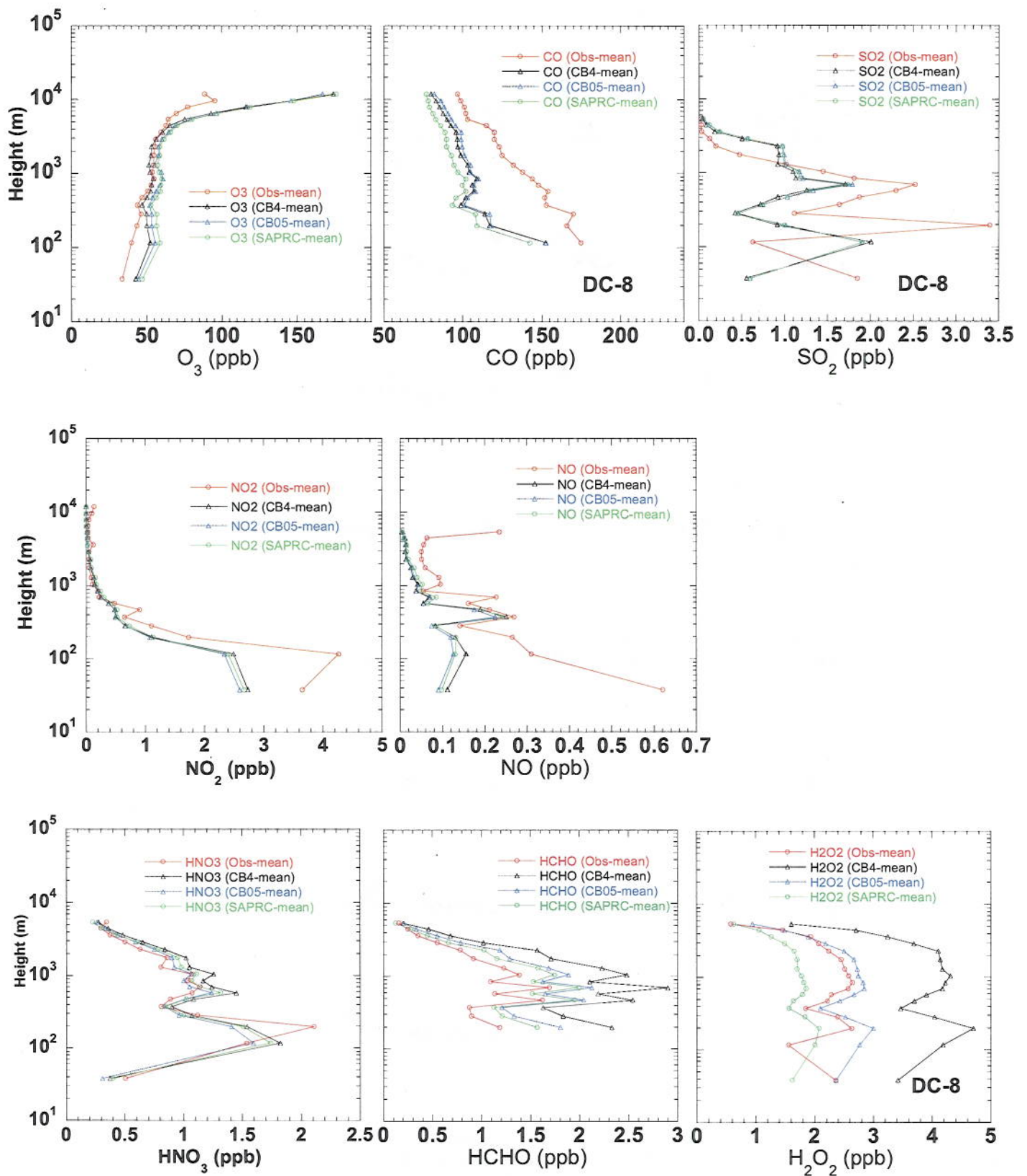


Figure 6. The same as Figure 3 but for vertical O_3 , CO , H_2O_2 , HNO_3 , NO_2 , NO , SO_2 and $HCHO$ profiles based on DC-8.

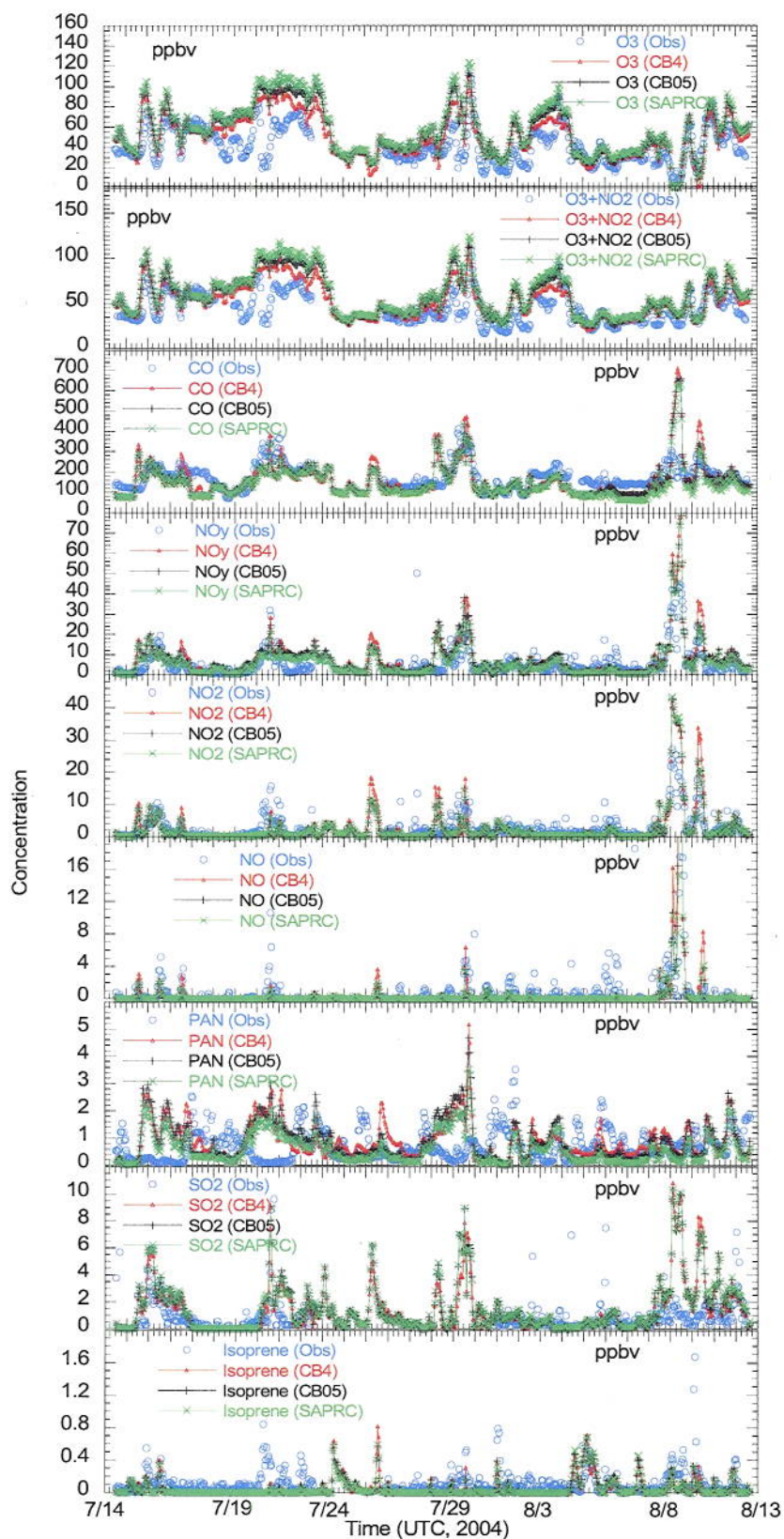


Figure 7. Time series comparisons of model predictions and observations for different species on the basis of ship measurements.